

This dissertation has been 65-3808  
microfilmed exactly as received

THOMPSON, Robert Wayne, 1937-  
THE EFFECT OF NITROGEN ON THE STRAIN  
AGING AND BRITTLE-DUCTILE TRANSITION OF  
VANADIUM.

Iowa State University of Science and Technology  
Ph.D., 1964  
Engineering, metallurgy

University Microfilms, Inc., Ann Arbor, Michigan

THE EFFECT OF NITROGEN ON THE  
STRAIN AGING AND BRITTLE-DUCTILE TRANSITION OF VANADIUM

by

Robert Wayne Thompson

A Dissertation Submitted to the  
Graduate Faculty in Partial Fulfillment of  
The Requirements for the Degree of  
DOCTOR OF PHILOSOPHY

Major Subject: Metallurgy

Approved:

Signature was redacted for privacy.

In Charge of Major Work

Signature was redacted for privacy.

Head of Major Department

Signature was redacted for privacy.

Dean of Graduate College

Iowa State University  
Of Science and Technology  
Ames, Iowa

1964

## TABLE OF CONTENTS

	Page
I. INTRODUCTION	1
II. REVIEW AND ANALYSIS OF LITERATURE	4
III. SPECIMEN PREPARATION	25
IV. EXPERIMENTAL PROCEDURES	32
V. PRESENTATION AND DISCUSSION OF EXPERIMENTAL RESULTS	39
VI. SUMMARY	90
VII. BIBLIOGRAPHY	93
VIII. ACKNOWLEDGEMENTS	102

## I. INTRODUCTION

During the past decade there has been a growing demand for the refractory metals for special applications in the technologies of nuclear reactors, aerospace and basic research. The basic reason for the interest in these metals is quite simple since their relatively high melting points suggest good structural strengths at high temperatures; however, the extreme reactivity of these metals to atmospheric gases at elevated temperatures presents severe oxidation and embrittlement problems.

Although ferrovanadium has been used as an alloying element in steel for many years, vanadium has become available in the unalloyed state only within the last 10 to 15 years. Vanadium, being a byproduct of the uranium industry, is now available in large quantities because of the great demand for uranium in nuclear energy applications (1). However, because of this recent availability, the properties of vanadium are not well known and thus few applications have as yet been made.

It is unfortunate that one property for which vanadium is generally known is its tendency toward the formation of molten vanadium pentoxide upon exposure to air at the relatively low temperature of  $675^{\circ}\text{C}$ . While this often may result in cato-

strophic failure of the material, this very characteristic, however, may also be one of its more important properties since the oxidation resistance of siliconized vanadium-columbium alloys has been attributed to the formation of a molten oxide with self healing properties (2).

Specialized applications might also be found where high electrical resistance and a relatively constant temperature coefficient of resistance are advantageous. Fabricability and weldability of vanadium are especially good compared to most of the other refractory metals. In addition, vanadium has by far the lowest density of the ten highest melting metals and its strength-to-weight ratio is therefore very favorable. However, in contrast to the effort expended on the other refractory metals comparatively little has been done in assessing the potential of vanadium. Hence it is necessary to determine the physical and mechanical properties of vanadium before many applications can be made.

Most of the body-centered cubic refractory metals are severely affected by the presence of small amounts of the interstitial impurities nitrogen, oxygen, carbon and hydrogen; therefore a study of the effects of interstitials on the mechanical properties of vanadium would be of interest. Of

the interstitials most commonly present in the refractory metals, nitrogen and oxygen are generally considered to have the most pronounced effects on the mechanical properties (3). No thorough study has been made on the effects of nitrogen on vanadium although there are some indications that it may have considerable influence on the deformation behavior of vanadium. For these reasons an examination of the effect of nitrogen on the mechanical properties of vanadium would be of considerable importance.

The intent of this investigation was to examine the role of nitrogen in the plastic behavior and brittle-ductile transition of vanadium and to relate these observations to current theories. Through a study of the elevated temperature mechanical behavior as evidenced by the strain aging phenomenon and the low temperature mechanical behavior as evidenced by the onset of embrittlement, it is hoped that a clearer concept into the mechanisms by which nitrogen affects the deformation characteristics of vanadium will be obtained.

## II. REVIEW AND ANALYSIS OF LITERATURE

The discussions in this section are intended to provide a background for understanding the mechanical behavior of the body-centered cubic metals and to allow a critical analysis of the experimental findings gathered during the course of this investigation. For convenience, this discussion will be divided into two sections. In Section A the general effects of the dislocation-interstitial atom interaction on the physical and mechanical properties will be presented, with particular emphasis being placed on the phenomenon of strain aging. Section B will be concerned primarily with the current theories of flow and fracture in body-centered cubic metals insofar as they pertain to the brittle-ductile transition.

### A. Dislocation-Solute Atom Interactions

The physical nature of a dislocation indicates there is a large strain energy associated with it. Around an edge dislocation, for example, the atoms above the slip plane are in compression while those below the slip plane are in tension. This strain energy can be relieved by the segregation of solute atoms to the dislocations, the larger substitutional atoms occupying positions in the expanded region, the smaller

ones taking positions in the compressed region and the interstitial atoms migrating to sites just below the extra half plane. This reduces the strain energy of the crystal and also the strain energy associated with the formation of solid solution.

Four general types of interactions between solute atoms and dislocations have been postulated: (i) elastic (4), (ii) chemical (5), (iii) electrical (6) and (iv) geometrical (7). Of these, it appears that the elastic interaction is the most important since Cottrell (6) has calculated that this interaction would be several times stronger than the other interactions.

The formation of an atmosphere around an edge dislocation due to hydrostatic interactions has been treated quantitatively by Cottrell and Bilby (8). They derived an expression for the number of solute atoms which will migrate to a unit length of dislocation in time,  $t$ , at a temperature,  $T$ , to reduce the strain energy of the system, which is given by:

$$n(t) = \alpha n_0 \left( \frac{ADt}{kT} \right)^{2/3}$$

where  $n_0$  is the average concentration of solute in solid solution,  $A$  is a constant which depends upon the interaction between the solute atoms and the dislocations,  $\alpha$  is a constant

and  $D$  is the diffusion coefficient of the solute. This expression, however, applied only to the initial stages of aging since no allowance was made for the depletion of solute during the course of strain aging. Harper (9) has modified this equation by suggesting that in the later stages of aging account should be taken of the competition between partially filled atmospheres by letting the rate of removal of the solute atoms be proportional to the concentration left in solid solution at any instant. Thus letting  $q = n(t)/n_0$ , he has shown that aging should follow the equation

$$\frac{dq}{dt} = (1-q)\alpha \left(\frac{ADt}{kT}\right)^{2/3}.$$

This equation was found to describe aging almost to complete saturation of the dislocations and the activation energy of the process was shown to be equal to the activation energy for the diffusion of the solute that was present (9, 10, 11, 12).

Nabarro (13) pointed out that due to the tetragonal distortion around an interstitial solute atom in body-centered cubic metals there should also be an interaction with the shear stresses around a screw dislocation. As was shown by Cochardt et al. (14) this should also lead to the formation of an atmosphere around screw dislocations.

There is considerable experimental evidence for the

segregation of solute atoms to dislocations. The first observations of dislocations within crystals were made by Hedges and Mitchell (15, 16) in which dislocations in silver bromide crystals were decorated with photolytic silver. After an annealing treatment and exposure to light, the colloidal silver segregated to the dislocation lines and could be examined in the optical microscope. This technique has been extended to the other halide salts (17) and to silicon (18). The decoration in silicon is accomplished by diffusing copper into the crystal at  $900^{\circ}\text{C}$  so that upon cooling the copper precipitates along the dislocations. The decorated crystal is then examined optically, using infra-red illumination; the dislocation-free areas transmit the infra-red illumination, but the decorated dislocations are opaque.

Segregation of solutes along dislocations has also been observed by the techniques of transmission electron microscopy. Phillips (19) observed that dislocations were decorated with precipitates of carbides and nitrides after a dilute iron-carbon-nitrogen alloy had been slowly cooled from  $750^{\circ}\text{C}$ . Van Wijk and Van Dijk (20) observed individual "hills" in subgrain ridges in iron-0.05% carbon steel. These hills were interpreted to correspond to individual dislocations with intersti-

tial atmospheres. The observation of "mounds" at dislocations by Phillips (21) was also attributed to the segregation of carbon and nitrogen to form interstitial atmospheres in agreement with the views of Van Wijk and Van Dijk. Impurity segregation at dislocations in quenched specimens of tungsten has also been observed (22).

Plastic flow in the body-centered cubic transition metals is highly dependent upon the presence of interstitial impurity atoms. Interactions between dislocations and interstitial impurities become especially evident in the intermediate temperature region (0.1 to 0.2  $T_m$ ). These interactions are manifestations of the phenomenon commonly known as strain aging. Lubahn (23) has summarized the mechanical effects associated with strain aging as follows:

- (i) The return of the yield point after an appropriate straining and aging treatment.
- (ii) The occurrence of discontinuous yielding or serrated stress-strain curves.
- (iii) A maximum in the ultimate tensile strength versus temperature curve.
- (iv) A minimum in the strain rate sensitivity versus temperature curve.

Aging for times longer than that required to produce the return-of-yield point can also result in an additional effect known as strain-age hardening. Strain-age hardening produces an additional strengthening effect which results in raising of the flow curve (24).

Strain aging was first observed in mild steels, and for some time, it was thought that this phenomenon was peculiar to this material. It is now known, however, that strain aging is quite common in the body-centered cubic metals, also occurs in the face-centered cubic and hexagonal close-packed metals (25), and is even found in such materials as silver chloride (26) and sodium chloride (27).

The most familiar strain aging characteristic is, no doubt, the return-of-yield point. It has already been shown that an interstitial impurity atom such as carbon or nitrogen will segregate to dislocations where it reduces not only the strain energy of the lattice but also the strain energy associated with solid solution formation. The influence of impurity atoms on the yield phenomenon can be explained as follows. Under an applied stress the dislocations will attempt to pull away from their impurity atmospheres, but the atmospheres exert a restraining force tending to pull them back

again. However, when a sufficiently large force is applied to the specimen plastic flow is produced by pulling the dislocations away from their atmospheres. Thus, as an increased stress is applied to a tensile specimen, the upper yield stress is reached at which point the restraining force of the atmosphere is overcome and once the dislocations have broken away from their atmospheres they can move through the lattice relatively unhindered. Clearly the applied force necessary to free the dislocation from its atmosphere is larger than the force needed to keep it in motion, hence the appearance of a yield point. If the specimen is strained beyond the yield point, unloaded and reloaded before the atmospheres have had sufficient time to reform, no yield point will appear upon reloading. However, if upon reloading sufficient time is allowed for diffusion of the impurity solute to occur, the atmospheres will reform and the yield point will reappear. This, then, is the strain-aged condition. The yield point and other strain aging effects can be suppressed or eliminated by removal of the responsible solute from solid solution. Cottrell and Leak (28) have shown that the rate of strain aging in low-carbon steels is dependent upon the amount of carbon and nitrogen in solution. Strain aging can be eliminated by removal of carbon

and nitrogen by treatment with moist hydrogen (29) or by the formation of a stable carbide or nitride (30, 31, 32).

The Cottrell model (4) also predicts the strong temperature dependence of the yield strength that is observed in the body-centered cubic metals. Thermal energy available to free the dislocation from its atmosphere decreases markedly with decreasing temperature. A greater applied external stress would then be necessary to move the dislocation resulting in the observed increase in yield strength.

Helsop and Petch (33) attributed the temperature dependence of the yield strength to an increase in the lattice frictional stress while Schoeck (34) has pointed out that a large increase in the jog density would account for the strong temperature dependency. These last two models should be relatively insensitive to impurity concentration while the Cottrell model requires the presence of interstitials. Consequently one should be able to decide between the Cottrell model and the other two by studying the yield strengths of very pure body-centered cubic metals. If the temperature dependency persists down to very low impurity levels it could be concluded that one of these "intrinsic" mechanisms is responsible. Conversely if a marked decrease occurs it would appear that

the Cottrell model gives the correct interpretation. Recent work by Stein et al. (35) on very pure iron single crystals shows a very marked reduction in the temperature dependence of the yield stress which gives strong support to the Cottrell mechanism.

Discontinuous yielding has been observed for metals at low temperatures up to as well as in the intermediate temperature region. The low temperature discontinuities are generally attributed to twinning (36) although hydrogen-induced strain aging has been reported to occur at  $-120^{\circ}\text{C}$  (37). The serrations associated with the strain aging phenomenon are thought to be due to alternate locking and unlocking of dislocations during plastic deformation (38).

A maximum in the ultimate tensile strength versus temperature curve is generally observed concomitant with serrations. Nabarro (13) has proposed the following explanation for the strain aging peak or blue brittleness region as it is referred to in iron. He reasoned that in this temperature region the pinning atmosphere diffuses along with the moving dislocations resulting in a "viscous drag" on the dislocations and producing an increase in strength. At higher temperatures the atmospheres become so dilute that essentially no locking

exists, while at lower temperature the interstitial atom mobility is so low that the atmosphere cannot diffuse along with the dislocation. The appearance of more than one peak (39, 40) is attributed to the presence of additional impurities capable of producing locking, and the ability to resolve these peaks is dependent upon the difference in mobility of the impurities involved.

These strain aging phenomena have been observed in vanadium by a number of investigators. Pugh (41) observed maxima in the tensile strength and strain hardening exponent and minima in the strain rate sensitivity and elongation at 400°C for calcium-reduced metal. Farrell (42) also found a maximum in the tensile strength and a minimum in elongation at this temperature. Eustice and Carlson (43) reported the appearance of serrations in the stress-strain curves between 140 and 180°C for iodide vanadium containing 600 ppm oxygen. Bradford and Carlson (44), studying the effects of oxygen in vanadium, observed that these serrations disappear at low oxygen concentrations but found evidence for strain aging at 350 to 400°C in metal containing 50 ppm oxygen.

From the above data it is quite evident that strain aging does occur in vanadium; however, none of the work to date identifies which impurity or impurities are primarily associated with this phenomenon in vanadium.

## B. Brittle-Ductile Transition

### 1. Historical sketch

The occurrence of brittle fracture in metals is not a new problem but has been recognized for a great many years. It first became evident when Bessemer steel began to be used as a structural metal in the 1860's, and as increased quantities of steel were used brittle fracture in engineering structures became more common. One of the first papers on brittle fracture reported the occurrence of fractures in Bessemer steel impacted under severe weather conditions (45). Thus as early as 1879 high strain rates and low temperatures were recognized to promote embrittlement.

Besides being of scientific interest brittle fracture is also of considerable economic importance since many failures have involved considerable loss of life and property as evidenced by the collapse of water standpipes, gasholders, storage tanks and bridges as reported by Shank (45). Undoubtedly the greatest stimulus to research on brittle fracture, however, came as a result of ship failures during World War II. Although ship casualties occurred in both welded and riveted construction the majority of failures were in welded ships. Many of these failures were due to faulty welding techniques;

however, perhaps even more serious was faulty design since these early structures were not redesigned with the change-over from riveting to welding. From examination of these failures investigators concluded that the brittle fracture was promoted by (i) low temperatures, (ii) rapid strain rates, (iii) multi-axial restraint, (iv) large size and (v) residual stresses.

## 2. Experimental observations

Brittle fracture is not only characteristic of steels but is found in many body-centered cubic metals and in some hexagonal close-packed metals but has not been observed in the face-centered cubic metals. Brittle fracture in the body-centered cubic refractory metals besides being promoted by the conditions listed previously for steels is extremely sensitive to the presence of the interstitial elements hydrogen, nitrogen and oxygen. All of the metals in Groups Va and VIa (V, Nb, Ta and Cr, Mo, W) undergo a brittle-ductile transition, the temperature of which is dependent upon the testing conditions and the type and quantity of interstitial atoms present. Schwartzberg et al. (46) and Hahn et al. (3) present comprehensive summaries of the effect of interstitial solutes on the brittle-ductile transition of the refractory metals. A comparison of some

values for the transition temperatures of these refractory metals is presented in Table 1.

Table 1. Tensile transition temperatures for the refractory metals

Metal	Transition temperature, °C	Reference
V	-110	Eustice and Carlson (43)
Nb	-200	Wessel <u>et al.</u> (39)
Ta	-240	Imgram <u>et al.</u> (47)
Cr	150	Weaver (40)
Mo	0	Bechtold and Scott (48)
W	300	Bechtold and Shewmon (49)

From the above table it is apparent that the Group VIA metals have a much higher transition temperature than the Group Va metals. In addition they are much more notch sensitive and the recrystallized structures generally have higher transitions than the same material in the wrought condition. The higher transition temperature of the recrystallized structure is generally attributed to segregation of interstitial atoms at grain boundaries. That Group Va metals are not as structure sensitive has been explained by their higher solubilities of interstitial solutes and therefore a much higher solute content would be required to develop a comparable degree of grain boundary segregation which would produce structure sensitivity (47).

The brittle-ductile transition characteristics of vanadium have been studied by several investigators. Roberts and Rogers (50) reported evidence to indicate that the low temperature brittleness of vanadium was associated with hydrogen embrittlement. They charged 0.035 in. diameter wires with 400 to 600 ppm hydrogen and tested specimens in tension in the cold-worked and recrystallized conditions. In both cases the hydrogenated wires were ductile at 150°C, brittle at room temperature and ductile again at -196°C although to a lesser extent than at 150°C. They suggested that the return of ductility at low temperatures may be associated with the ordering of hydrogen in the vanadium lattice. They also observed that a small amount of second phase hydride had little or no effect on the mechanical properties. Hydrogenated vanadium foils were found to exhibit (100) cleavage. Eustice and Carlson (43) observed no embrittlement in high purity hydrogen-free vanadium down to -196°C but found that the presence of only 10 ppm hydrogen was sufficient to cause embrittlement at -110°C over a limited temperature range. They noted that an increase in hydrogen content raised the brittle-ductile transition temperature and also that the transition temperature was shifted to higher temperatures with an increase in strain rate. It was

their conclusion that hydrogen embrittlement occurs as a result of the interaction of hydrogen atmospheres with dislocations, this interaction being a maximum over a critical temperature range which varies with strain rate and hydrogen concentration.

According to Clough and Pavlovic (51) commercially pure, calcium-reduced vanadium tested in tension exhibits cleavage fracture at  $-196^{\circ}\text{C}$  while ductile fracture is observed at  $-140^{\circ}\text{C}$  and above. They noted that both the  $\{100\}$  and the  $\{110\}$  planes were active cleavage planes with fractures nucleating and terminating at grain boundaries. Mechanical twinning occurred on  $\{112\}$  planes and only within one or two grains of a cleaved surface.

In a study of the tensile and bend properties of bomb-reduced and crystal-bar vanadium Loomis and Carlson (52) observed a brittle-ductile transition at  $-65 \pm 10^{\circ}\text{C}$  and  $-110 \pm 10^{\circ}\text{C}$ , respectively. This work indicated that the transition temperature is particularly sensitive to hydrogen, nitrogen and oxygen while the effect of carbon is somewhat less.

The embrittling effect of oxygen on the bend ductility of iodide vanadium was investigated by Bradford and Carlson (53). They observed no embrittlement in samples containing less than

1500 ppm oxygen; however above this value the transition temperature increased sharply with oxygen content.

Magnusson and Baldwin (54), upon examining the effects of strain rate on the low temperature properties of vanadium, observed no brittleness in tensile tests carried out as low as  $-196^{\circ}\text{C}$  and at speeds up to 19,000 in./in./min. Armstrong and Lund (55) found no completely brittle fracture down to  $-196^{\circ}\text{C}$  for zone-refined single crystals of vanadium tested in tension. Furthermore they reported extensive necking at all test temperatures.

From the above data concerning vanadium several conclusions may be drawn. Vanadium when sufficiently free of interstitial solutes shows no brittle-ductile transition. Hydrogen has a very pronounced embrittling effect even at concentrations as low as 10 ppm while oxygen causes embrittlement when present in concentrations exceeding 1500 ppm. Although no detailed studies have been made on the individual effects of nitrogen and carbon, from a comparison with the other refractory metals both would be expected to cause brittleness with nitrogen being the more potent (3).

### 3. Crack nucleation

Although the brittle fracture of metals has been studied

extensively for a good many years there is at present no universally accepted explanation for this phenomenon. It should be noted, however, that this low temperature brittleness appears to be associated with a strong temperature dependence of the resistance to plastic flow. The body-centered cubic metals, which are most susceptible to brittle fracture, exhibit a marked increase in the temperature dependence of the yield strength in the region where the ductility transition generally occurs while the face-centered cubic metals, for which no brittle-ductile transition is found, do not show this strong temperature dependence. The differences in the temperature dependence of the yield stress are generally attributed to dislocation pinning or an increase in the lattice frictional stress, both of which were discussed previously and will not be further elaborated here.

Early attempts to explain brittle fracture were made by Griffith (56) and Ludwik (57). Griffith postulated that microcracks were responsible for the observed low values of strength. According to his model microcracks are present in all materials and will propagate only when the free energy of the system is reduced by the growth of the crack. He considered only the surface energy increase and the elastic strain

energy decrease as the crack propagates and neglected the energy associated with plastic flow. Thus while this model may be adequate for a brittle material such as glass it does not provide reasonable answers for metals and does not consider the problem of crack nucleation. Ludwik proposed that cleavage fracture occurs in a metal when the flow curve intersects the fracture stress curve. He proposed that the fracture curve changed very little with temperature while the flow curve is found to be quite temperature dependent. According to Ludwik's analysis the flow curve lies below the fracture curve above the temperature of this intersection and ductile behavior should be observed; however below this temperature the flow curve is above the fracture curve and hence brittle fracture occurs. Although this is a useful approach it provides no information about the atomistic mechanisms involved.

Zener (58) proposed that crack nucleation is associated with plastic deformation. He suggested that when a slip band is blocked by some obstacle, such as a grain boundary or precipitate, very large tensile stresses can be developed which might exceed the cohesive strength of the matrix and produce a crack. He also proposed that cracks can be nucleated by the

coalescence of dislocations. Stroh (59) showed that dislocation pileups at grain boundaries can produce microcracks in support of Zener's hypothesis.

Cottrell (60) has suggested a somewhat different mechanism for nucleating cleavage cracks. He has shown how dislocations in two intersecting (110) slip planes in a body-centered cubic lattice can reduce their elastic energy by coalescing on a (001) cleavage plane to form a new dislocation. This new dislocation lies in the (001) cleavage plane and because of its large Burgers vector normal to the cleavage plane may be looked at as an elementary crack which can grow by the coalescence of additional pairs of dislocations. Stroh (61) has also postulated a mechanism whereby cracks might nucleate at subboundaries in single crystals.

There have been relatively few direct observations of crack nucleation in crystals. Generally complete fracture is observed, and although the fracture initiation source may be identified, the fracture mechanism is a matter of conjecture. Stokes and coworkers (62, 63, 64), however, have made an extensive investigation of crack nucleation during slip in MgO. They have shown that cracks are nucleated at the intersections of (110) slip bands. These cracks initially propagate along

the (110) slip plane but eventually switch to the (100) plane normal to the tension axis to produce complete fracture. They have also shown that the propagation of a crack can be interrupted by intersection with another slip band and that microcracks may form at the intersection of slip bands with grain boundaries. Honda (65) working with Fe-3% Si alloys also found microcracks to nucleate at slip band intersections.

Many of the metals which exhibit low temperature brittleness also deform by twinning at these temperatures, thus suggesting that twinning may be responsible for crack nucleation. Hornbogen (66) found evidence that the sudden formation of a twin can produce stress waves which, when reflected from some obstacle such as grain boundaries or other twins, could produce cleavage cracks. Crack nucleation at twin intersections in iron-silicon single crystals were observed by Hull (67) and Honda (65) and the formation of cracks at the intersections of twins with hydride platelets in columbium has been reported by McHargue and McCoy (68).

From metallographic examination of fractured specimens of the refractory metals, and especially the Group VIa metals, it has been noted that fractures in polycrystalline specimens usually start at grain boundaries and propagate almost entirely by transgranular cleavage (51, 69, 70, 71).

### III. SPECIMEN PREPARATION

#### A. Vanadium Metal

The vanadium used as a base material in this investigation was prepared by the iodide refining process as described by Carlson and Owen (72). A representative analysis of the base metal is given in Table 2.

Table 2. Representative analysis of iodide-refined vanadium

Element	Content, ppm	Element	Content, ppm
O	150	Cr	250
H	<1	Cu	40
N	<5	Fe	250
C	150	Mg	<15
Al	40	Mn	<20
Ca	<20	Ni	110
Si	<40	Ti	30

Oxygen, hydrogen and nitrogen were determined by vacuum fusion methods with the nitrogen also being determined by a modified Kjeldahl procedure. Carbon was determined in a Leco conductometric carbon determinator while the metallic impurities were determined spectrographically.

The crystal-bar vanadium was consolidated by arc melting on a water-cooled, copper-hearth furnace under an argon atmosphere which had been purified by gettering with zirconium.

## B. Tensile Specimens

The vanadium base metal was treated with calcium vapor to reduce the oxygen content similar to the method of Allen et al. (73). Small pieces of iodide-refined vanadium were placed in a tantalum crucible along with a small amount of high purity calcium metal and welded shut under a helium atmosphere. This crucible was then enclosed in inconel and heated at 1100°C in a muffle furnace for four days. After this treatment the excess calcium and the calcium oxide were removed from the vanadium by dissolution with dilute acetic acid. In this manner the oxygen content was reduced to about 20 ppm.

Nitrogen was added to the test alloys through the use of a master alloy. The master alloy was prepared by arc-melting the vanadium under an atmosphere of argon and purified nitrogen, the nitrogen being added intermittently to the melting chamber as it was absorbed by the vanadium. In this manner a master alloy was prepared containing 5.6 weight per cent nitrogen. The test alloys were then prepared by arc-melting measured amounts of the master alloy with the base metal. The arc-melted ingots, homogenized by repeated melting, were swaged at room temperature into 0.188 in. diameter rods and machined into tensile specimens. Fig. 1 shows the dimensions

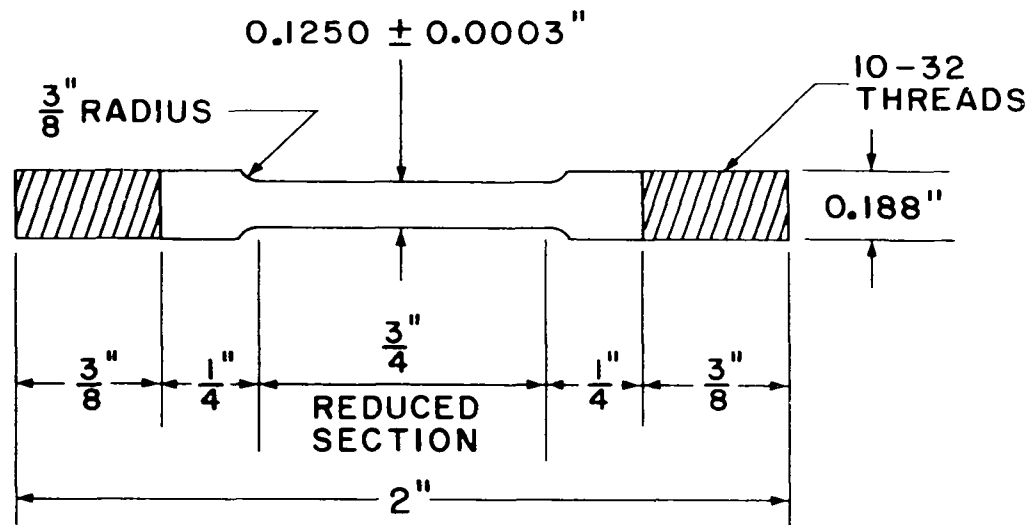


Figure 1. Tensile test specimen

chosen for the tensile specimens used in this investigation. After completion of the machining operations the specimens were cleaned with trichloroethylene, dried with acetone, annealed for one hour at 1000°C in a dynamic vacuum of  $3 \times 10^{-6}$  Torr and slowly cooled to room temperature. This procedure produced a specimen with a bright mirror-like finish and a recrystallized structure with a uniform grain size of 45 to 50 grains per square millimeter. Samples for analysis were removed from the specimens subsequent to testing.

### C. Bend Specimens

Individual additions of both nitrogen and carbon were made in this study. Specimens prepared with nitrogen additions were utilized in both the poly- and monocrystalline form while specimens containing carbon additions were tested only in the polycrystalline form.

#### 1. Polycrystalline specimens

Test alloys were prepared from measured amounts of the base metal and the master alloy. The nitrogen master alloy was the same as described earlier while the carbon master alloy was prepared by arc-melting vanadium and spectroscopically pure carbon to form an alloy which was shown by analysis to contain

### 3.3 weight per cent carbon.

Arc-melted buttons containing over 1000 ppm carbon and all the alloys containing nitrogen were jacketed in mild steel and rolled at 650°C into 0.070 in. thick sheets. Bend specimens measuring 1 in. x  $\frac{1}{4}$  in. were cut from these sheets, surface ground to a thickness of 0.050 in., electropolished to a final thickness of 0.045 in. in a 10% HCl-H<sub>2</sub>O solution, annealed at 1000°C in a dynamic vacuum of  $3 \times 10^{-6}$  Torr and cooled slowly to room temperature. This procedure resulted in a recrystallized structure with 25-30 grains per square millimeter.

## 2. Monocrystalline specimens

Single crystals approximately  $\frac{1}{2}$  in. in diameter and 3 in. long were prepared in an arc-zone melter shown schematically in Fig. 2. Crystal growth was carried out under a zirconium-gettered argon atmosphere. The ingot was withdrawn at a speed of  $\frac{1}{2}$  in. per hour and a current of 140 amps at 15 volts was used. Bend specimens were cut from these crystals, electropolished to 0.045 in. thickness and heat treated as described above.

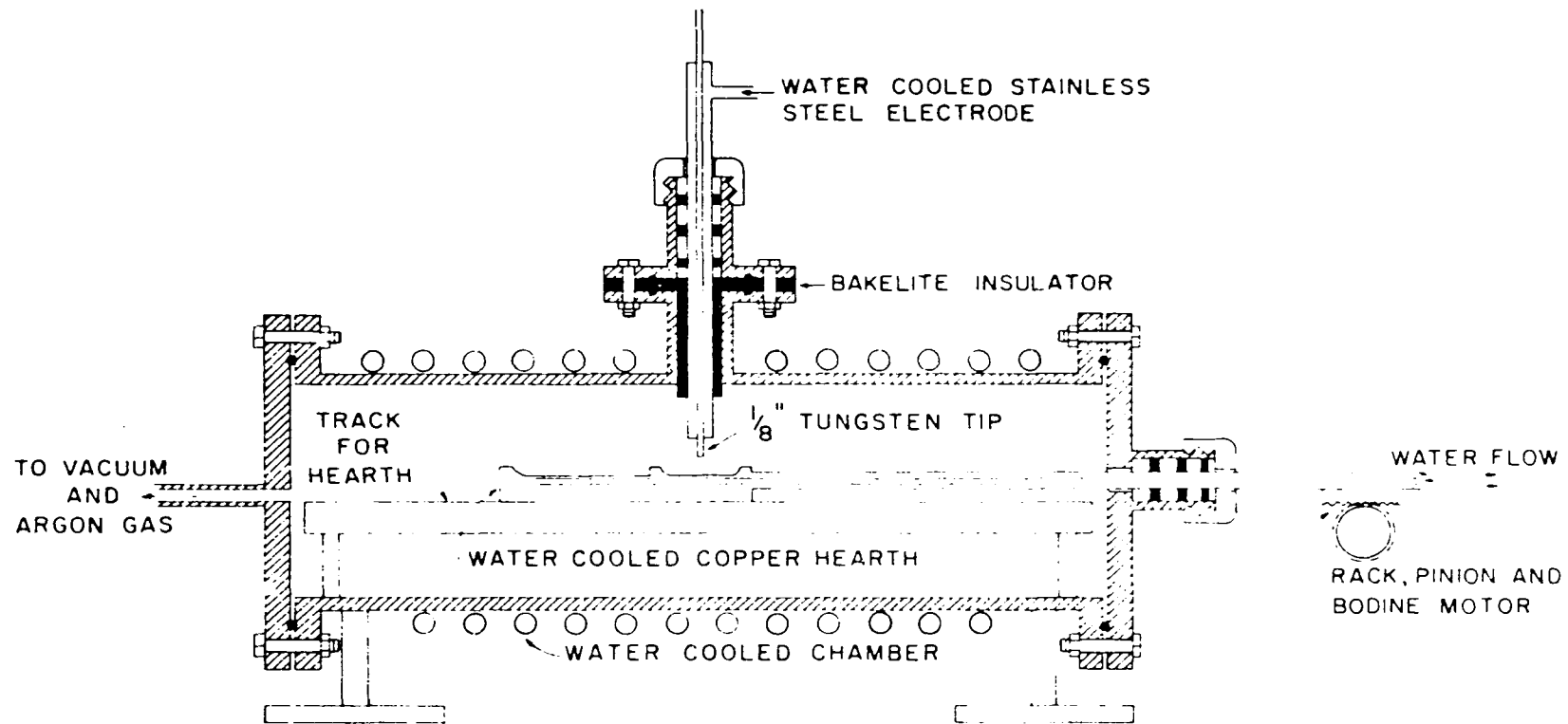


Figure 2. Schematic diagram of the arc-zone melting apparatus used for the preparation of vanadium single crystals

#### D. Extrusion Specimens

Approximately four pounds of iodide refined vanadium in the crystal bar form was cut into small pieces, thoroughly mixed, electron beam melted into a  $1\frac{1}{2}$  in. diameter ingot, rod rolled to 1 in. diameter and cut into 1 in. lengths. These specimens were recrystallized at  $1000^{\circ}\text{C}$  for 2 hours in a dynamic vacuum of  $3 \times 10^{-6}$  Torr and slowly cooled. This procedure resulted in specimens containing 120 ppm nitrogen and a grain size of 65-70 grains per square millimeter.

#### IV. EXPERIMENTAL PROCEDURES

The experimental methods employed in this investigation were selected upon consideration of (i) reproducibility of testing conditions, (ii) ease of specimen preparation and (iii) comparison with previous studies.

##### A. Tensile Tests

The tensile machine employed was a Riehle Model FS-10 Universal Screw Power Testing Machine equipped with a load deformation autographic recorder. The load indicating unit consisted of a horizontal balance beam and a movable poise controlled by a differential transformer. Elongation of the specimens was found from crosshead motion which was measured by a Riehle RD-5A deflectometer.

The specimens were loaded through spherically-seated balls which assisted in providing axial alignment. These balls were seated in adapters which were threaded onto 7/8 in. diameter spherically-seated pull rods. Temperature measurements were made with two chromel-alumel thermocouples. The maximum temperature gradient along the specimen was 3°C. Above 250°C the specimen chamber was enclosed with two concentric cylinders and a slight positive pressure of argon was

maintained around the specimen to reduce atmospheric contamination. A schematic diagram of the test chamber is shown in Fig. 3. The complete chamber was fabricated from stainless steel.

All specimens, unless otherwise noted, were tested at a crosshead speed of 0.01 in. per minute. Strain-rate sensitivity was determined by testing at 0.01 in. per minute and then momentarily changing the crosshead motion to 0.1 in. per minute.

#### B. Bend Tests

All specimens containing nitrogen additions were tested on the apparatus shown schematically in Fig. 4. The low temperatures were obtained by manually regulating the flow of liquid nitrogen through the hollow copper supporting block and the double-walled chamber. The specimens were bent by a plunger rod with a 1/16 in. end radius moving at a constant rate of 0.050 in. per minute. The deflection of the specimen was measured by means of a dial gauge in contact with the plunger.

The vanadium-carbon alloys were tested on the apparatus shown in Fig. 5. Temperatures down to  $-180^{\circ}\text{C}$  were maintained by a Brown temperature controller operating solenoid valves

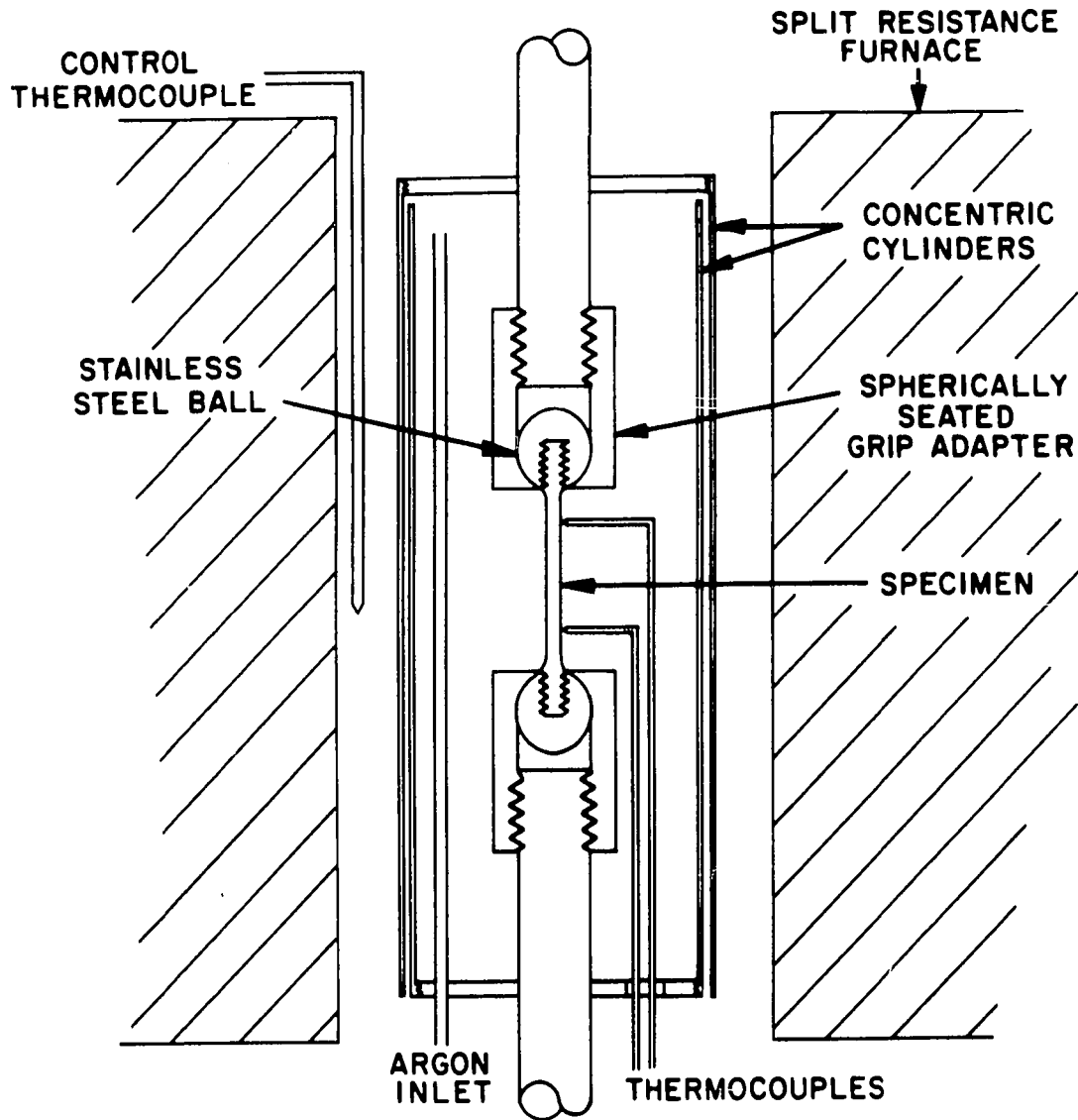


Figure 3. Schematic diagram of the tensile testing chamber

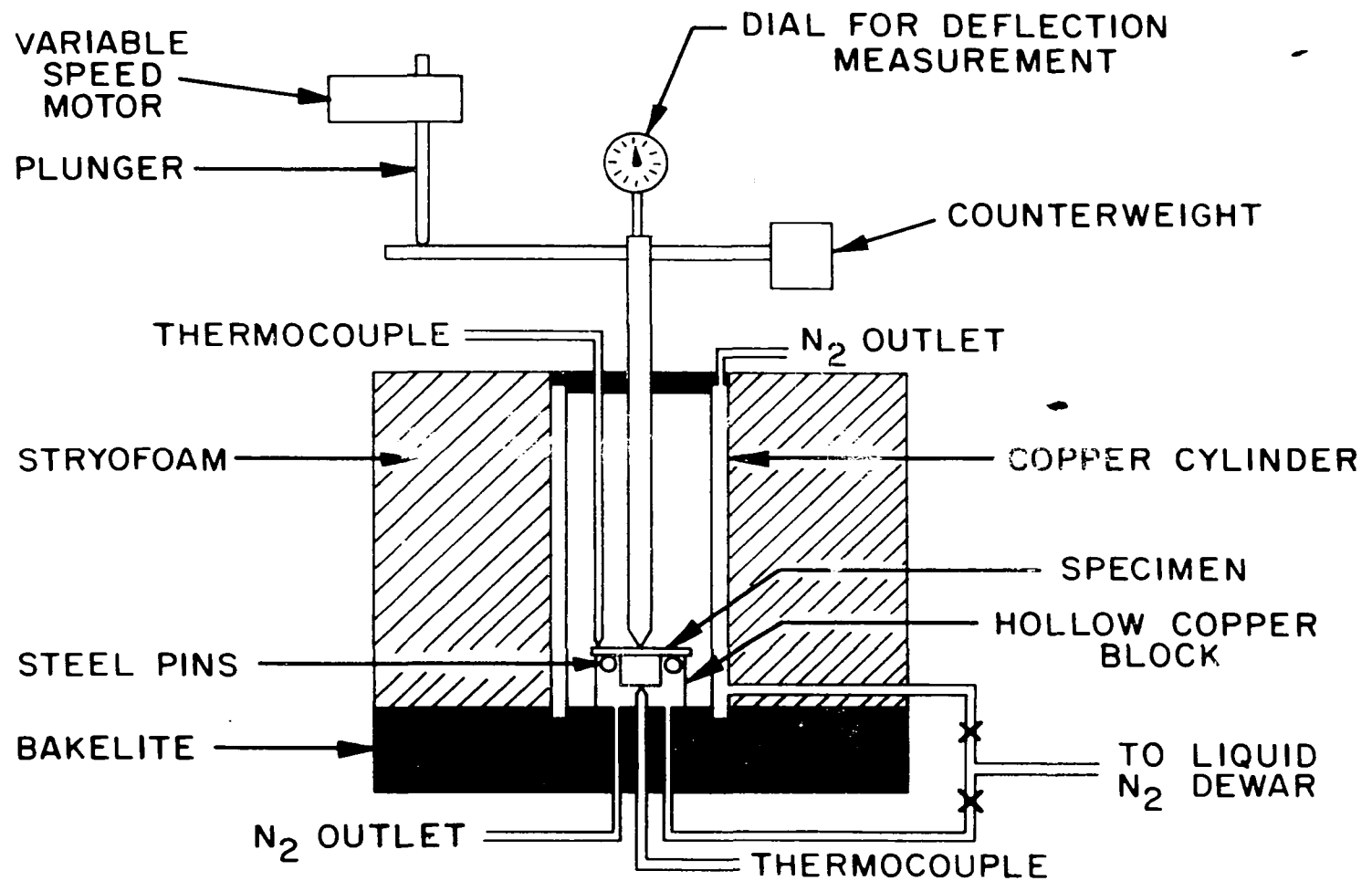


Figure 4. Schematic diagram of the bend testing apparatus used for vanadium-nitrogen alloys

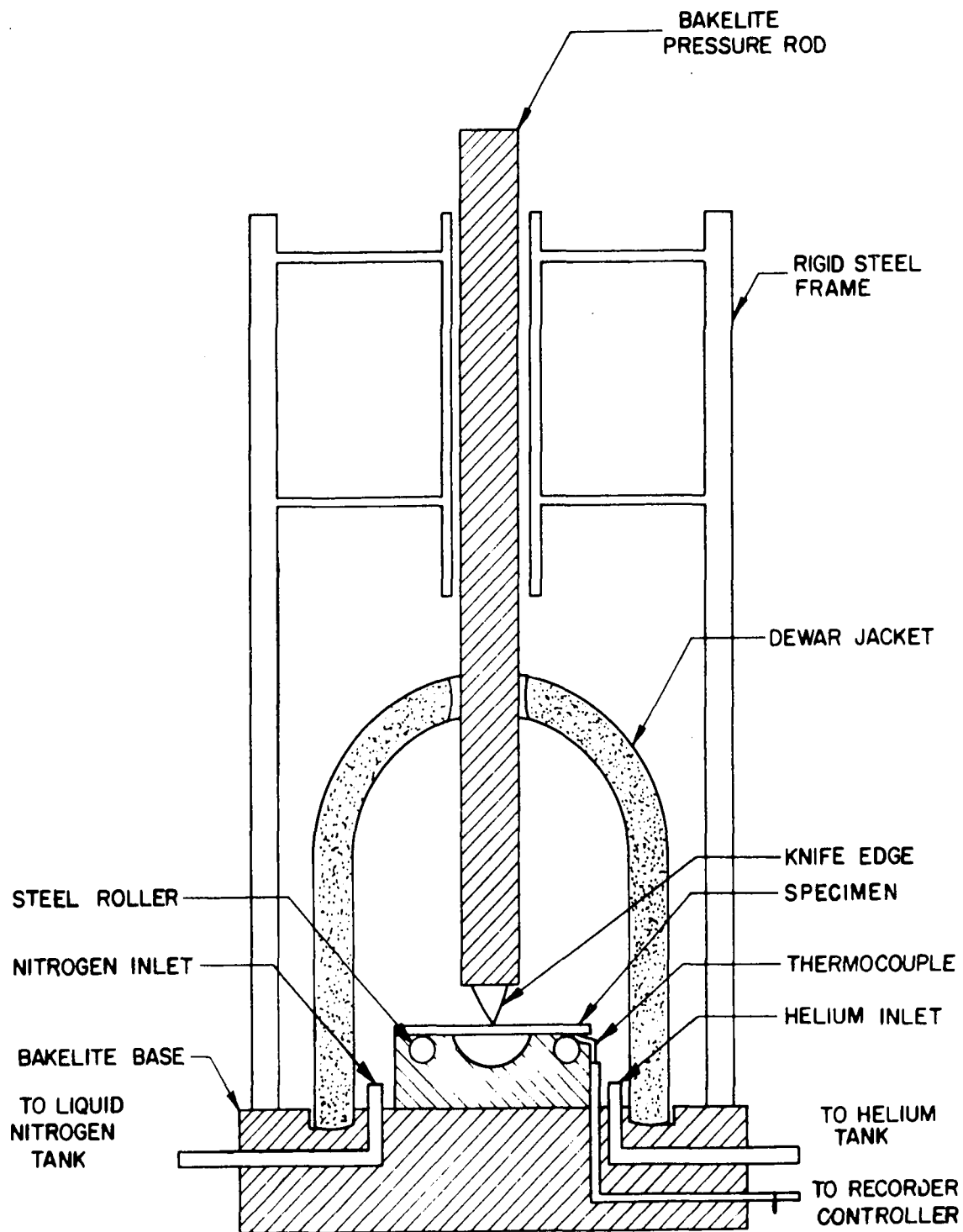


Figure 5. Schematic diagram of the bend testing apparatus used for vanadium-carbon alloys

which alternately forced liquid nitrogen or warm helium into the test chamber. Bend tests at  $-196^{\circ}\text{C}$  were made by placing a stainless steel cup in the system and immersing the specimen, holder and plunger tip in liquid nitrogen. The plunger was forced downward at a constant speed of 0.01 in. per minute by a Tinius-Olsen testing machine equipped with an X-Y recorder.

#### C. Hardness

Hardness measurements were determined on a Tukon micro-hardness tester equipped with a diamond pyramid indenter. All hardness values reported in this investigation are in DPH (Diamond Pyramid Hardness) units.

#### D. Extrusion

Vanadium billets 1 in. in diameter and 1 in. in length were extruded in a Dynapak impact forming machine. All extrusions were performed on unclad recrystallized billets using a graphite coating as a lubricant. An extrusion ratio of 12.5 to 1 was employed at a ram speed of about 200 in. per sec. In all cases the extruded rod exhibited very good flow characteristics.

### E. Metallography

The metallographic specimens were mounted in Bakelite and hand ground through 600 grit paper. The remainder of the surface preparation was then done on a Syntron vibratory polisher. The specimens were treated with Linde A powder on a wax lap and given a final polish with Linde B on a microcloth lap. Etching was done by immersion in a solution of 50 parts H<sub>2</sub>O, 10 parts HF, 5 parts H<sub>2</sub>SO<sub>4</sub> and 5 parts HNO<sub>3</sub> for a time of from 2 to 5 minutes.

## V. PRESENTATION AND DISCUSSION OF EXPERIMENTAL RESULTS

### A. Strain Aging

The term "strain aging" is used to cover a wide variety of effects in which some aging process takes place as a result of plastic strain. In general, the strain aging phenomenon is separated into those effects which occur after straining and are called "static strain aging" and those effects which occur simultaneously with straining, referred to as "dynamic strain aging". The general features of strain aging can be summarized into two types of effects: (i) a strengthening or raising of the flow curve and (ii) the reappearance of a yield point and/or the occurrence of serrations in the stress-strain curve.

There are several properties of a material which have to be used to study strain aging, such as electrical resistivity, internal friction, notched bar impact strength, hardness, yield-point return, the occurrence of serrated stress-strain curves, yield and tensile strengths. In this investigation tension tests were employed and consequently several of the above properties were amenable to study.

Since the object of this portion of the investigation was to study the effect of nitrogen on the strain aging of

vanadium, and both hydrogen and oxygen have been reported to cause strain aging, it was deemed desirable to reduce these impurities to a level where they would not interfere with or mask the effects due to nitrogen. Hydrogen was found to present no particular problem due to its high mobility at elevated temperatures and was eliminated during recrystallization of the specimens in a dynamic vacuum. Oxygen was reduced to a low level by exposing the vanadium to calcium vapors at 1100°C for four days. Chemical analysis of various specimens given identical deoxidation treatments are presented in Table 3.

Table 3. Effect of calcium deoxidation on the purity of vanadium

PPM oxygen	
Before treatment	After treatment
370	25
385	20
310	15
420	20
1190	10
170	20
345	15
525	20
255	35
540	15
710	15

1. Dynamic strain aging

A thorough study of the mechanical properties of iodide-refined vanadium as a function of nitrogen content and temperature was carried out to determine the extent to which these properties are altered by the strain aging phenomenon. The ranges of investigation were from 50 to 1160 ppm nitrogen and 25 to 550°C. The strain rate, calculated from the crosshead motion and the length of the reduced section, was 0.00022 in. per in. per second unless otherwise specified.

a. Ultimate tensile strength      The tensile property that was found to exhibit the most pronounced strain aging effect was the ultimate tensile strength. As can be seen from Fig. 6 the tensile strength versus temperature plots show minima in the strength around 200°C and maxima around 400°C. It should also be noted that these extreme temperatures are found to be independent of nitrogen content. The magnitude of the strain aging effect increases with increasing nitrogen content as seen from Fig. 7 where the difference in strength between the maximum and minimum of each curve is plotted versus nitrogen content. The maximum in the ultimate tensile strength coincides with the temperatures found for the occurrence of serrations in the stress-strain curves, the maximum

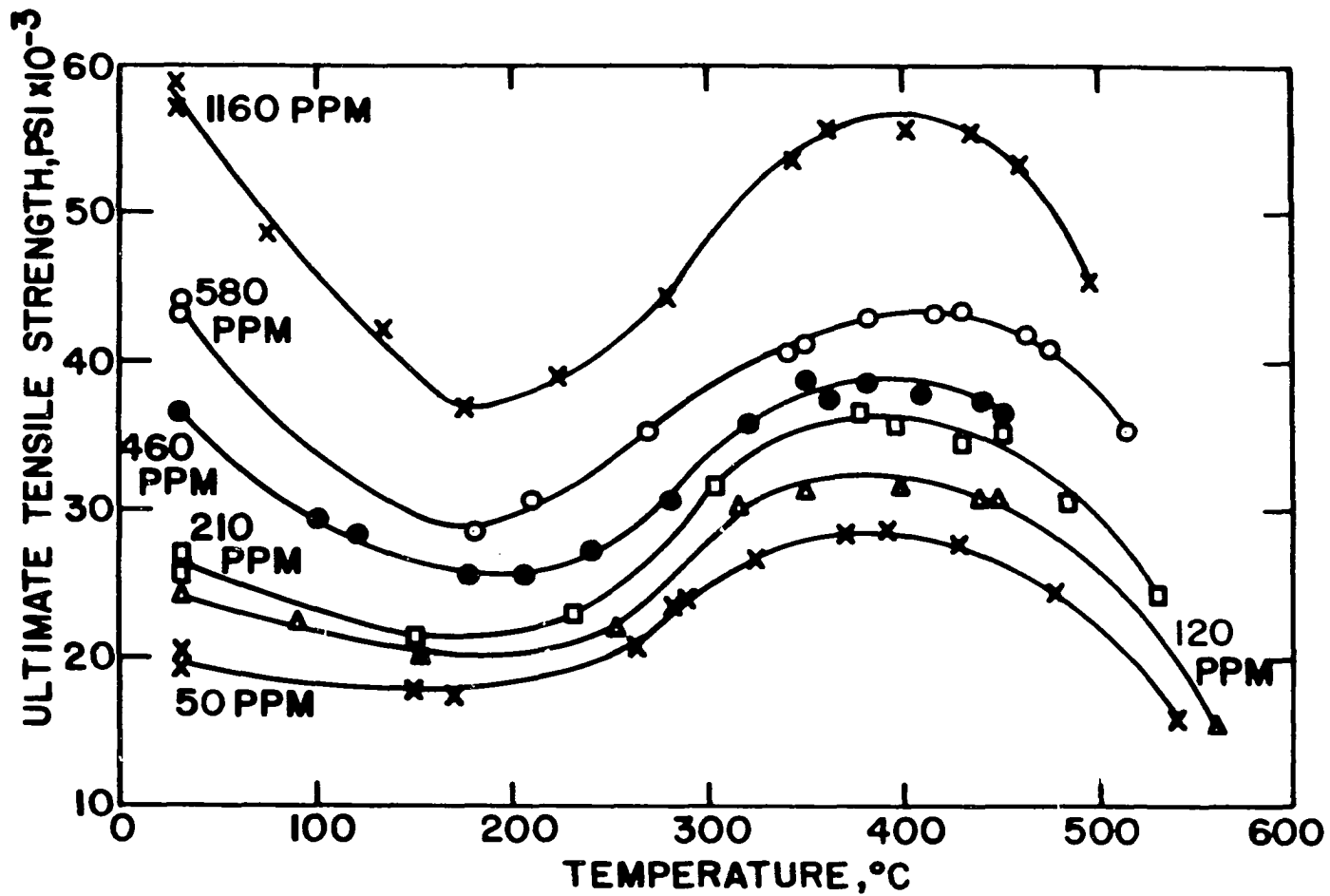


Figure 6. Influence of temperature on the ultimate tensile strength of vanadium

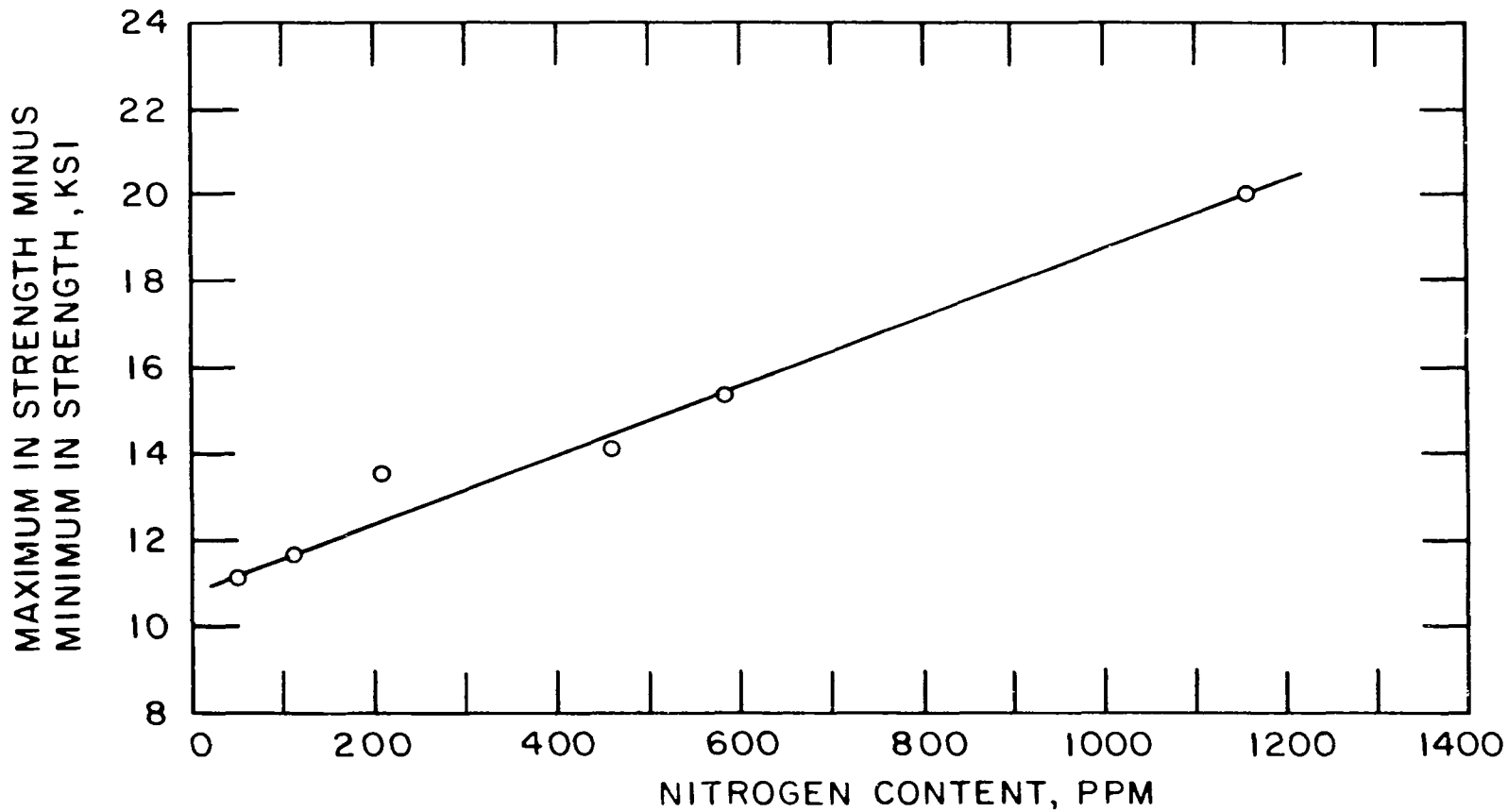


Figure 7. Effect of nitrogen on the magnitude of the strain-aging peak

in the strain hardening exponent, the slight maximum in the yield strength, the minimum in uniform elongation and the minimum in the strain rate sensitivity. These effects will be discussed later.

b. Yield strength      The yield strength versus temperature curves are shown in Fig. 8. The values used for this parameter were the lower yield stress, or if no yield point was present, the 0.2% offset stress. The maxima in the yield strength curves also occur at 400°C but are much less pronounced than the corresponding maxima in the tensile strength. From Figs. 6 and 8 it can be seen that for the initial portion of the curves the strength becomes increasingly temperature dependent with increasing nitrogen content.

c. Strain hardening exponent      When the tensile data are plotted as true stress versus true strain on logarithmic coordinates, a straight line relationship results, the slope of which is a measure of the rate of work hardening of the specimen. The quantity so defined, the strain hardening exponent is given by:

$$m = \left( \frac{\log \sigma}{\log \dot{\epsilon}} \right)_{\dot{\epsilon}, T}$$

where  $\sigma$  is the true stress,  $\epsilon$  the true strain and  $\dot{\epsilon}$  the strain rate. In general the strain hardening is expected to

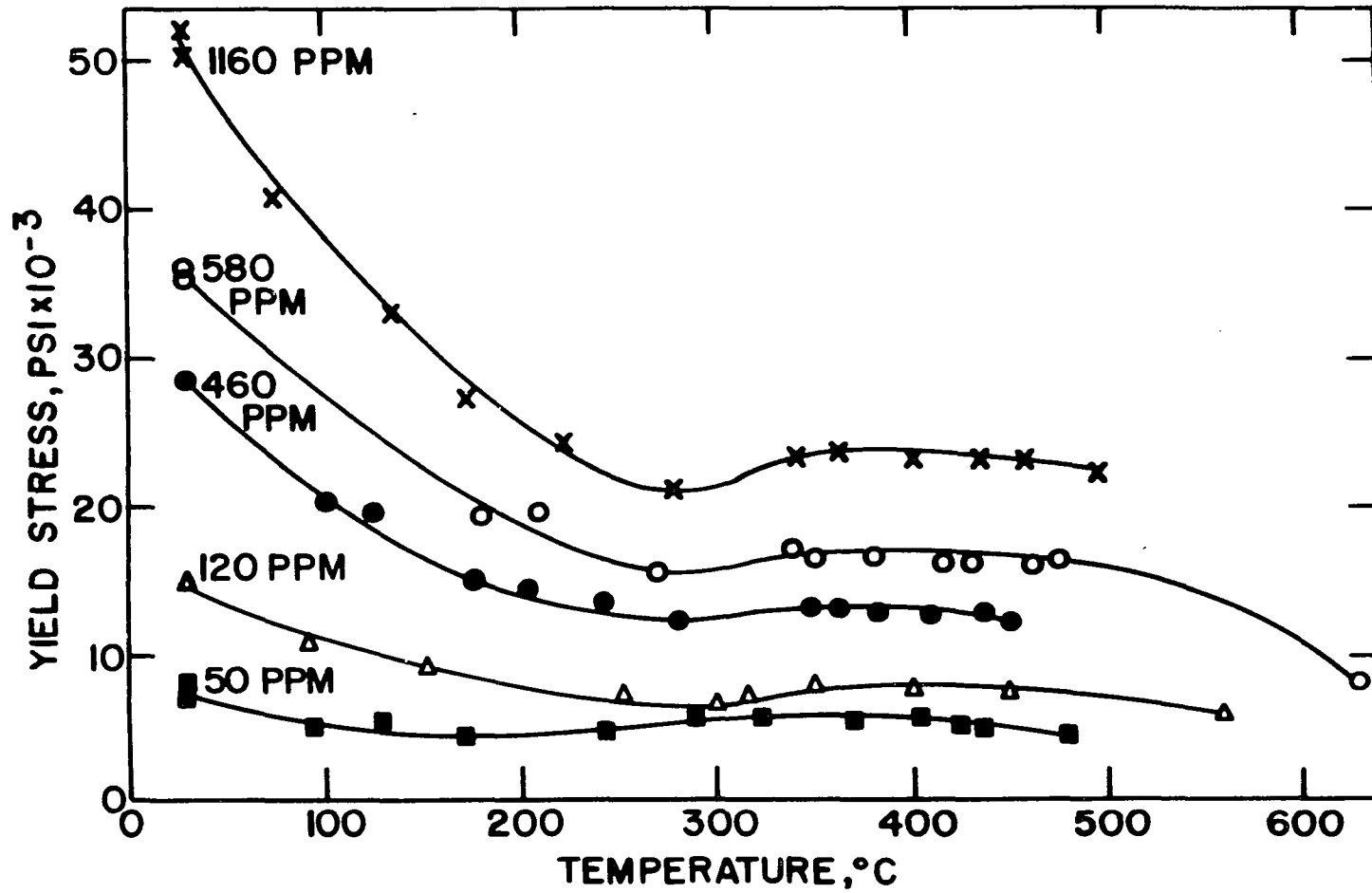


Figure 8. Influence of temperature on the yield strength of vanadium

decrease continuously with increasing temperature since at higher temperatures dislocation rearrangement is facilitated; hence stress concentrations are relieved and the work hardening rate decreases. The data shown in Fig. 9, however, do not follow this prediction but instead show a distinct maximum at about 400°C. This type of behavior is also noted in low-carbon steel where it was shown that the dislocation density in a specimen deformed in the strain-aging region was an order of magnitude greater than that in one deformed at room temperature to the same strain (74). A high dislocation density in this region is consistent with the high work-hardening rate observed.

d. Strain-rate sensitivity      If the strain rate is suddenly changed during a tensile test a vertical shift in the flow curve is usually observed, the flow curve for the faster rate being slightly above the curve for the slower rate. The flow stress depends both on the strain and the strain rate, and a quantity called the strain-rate sensitivity is defined as

$$n = \left( \frac{\log \sigma_1 / \sigma_2}{\log \dot{\epsilon}_1 / \dot{\epsilon}_2} \right)_{\epsilon, T} .$$

The temperature dependence of the strain rate sensitivity is related to a diffusional process which decreases the flow

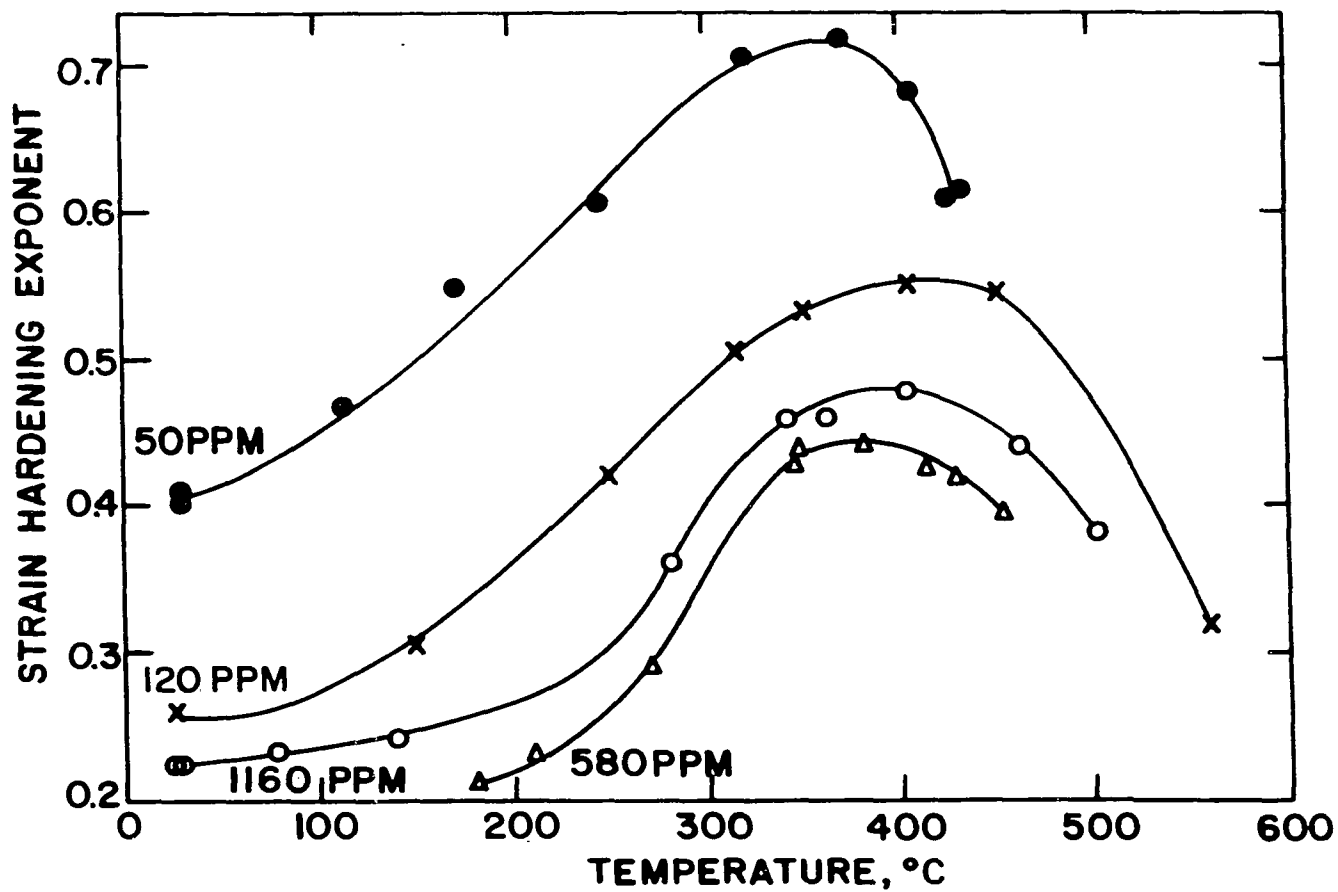


Figure 9. Effect of temperature on strain hardening of vanadium

stress by dislocation rearrangements. High strain rates reduce the time for rearrangements to occur, the effect being more pronounced at higher temperatures where diffusion is faster. Hence a continuous increase in strain-rate sensitivity with temperature is expected. This continuous increase has been reported in the case of platinum where the strain-rate sensitivity was found to be proportional to the absolute temperature (75). As is characteristic of a material which exhibits strain aging, the strain-rate sensitivity of vanadium shows a minimum in the strain aging region as shown in Fig. 10. The strain-rate sensitivity is observed to decrease since increasing the strain rate reduces the time for strain aging to occur; however, as the temperature is increased this reduction is overcome by the increased diffusivity of the interstitials and the strain-rate sensitivity again increases. It should be noted that the strain-rate sensitivity is negative in the 300 to 500°C range which shows that the specimens deform at a lower applied stress when strained at a higher rate. A negative strain-rate sensitivity was found for all specimens studied regardless of nitrogen content.

e. Ductility All specimens were ductile at the temperatures tested and necked down to a reduction in area of

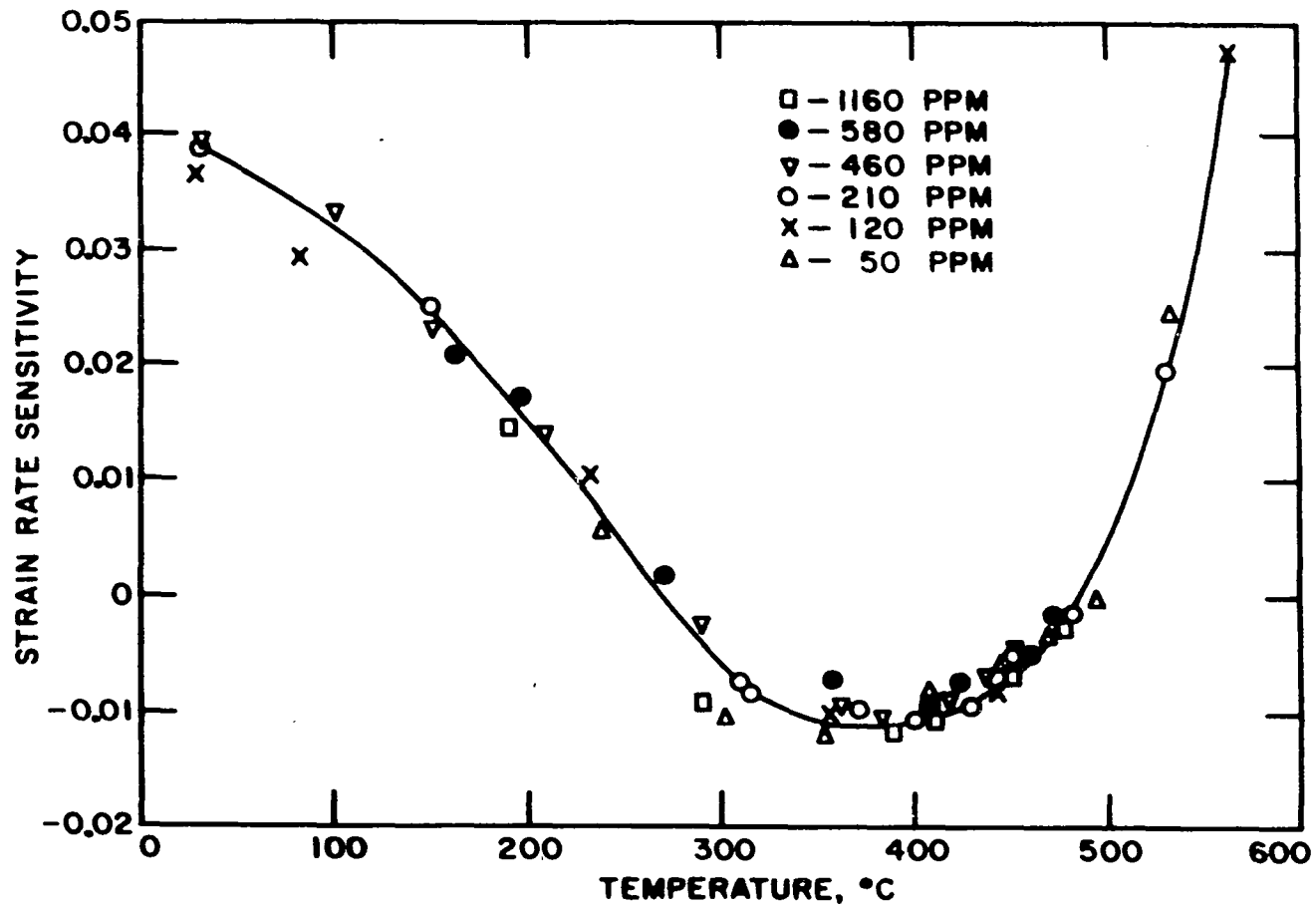


Figure 10. Variation of strain-rate sensitivity with temperature

nearly 100 per cent; hence no calculations were made for this parameter. An example of a typical tensile specimen is shown in Fig. 11. A minimum was found, however, in a plot of uniform elongation versus temperature as illustrated in Fig. 12.

f. Serrations In vanadium tested at room temperature there is only one yield discontinuity which is represented by the upper and lower yield points. At higher temperatures, however, a whole series of yield discontinuities occur which result in serrated stress-strain curves as illustrated in Fig. 13. This phenomenon of repeated yielding during a tensile test is attributed to dynamic strain aging. The interstitial solute has sufficient mobility to diffuse to moving dislocations and to slow their motion by forming anchoring atmospheres around them. The stress builds up rapidly causing the dislocation to break away from the anchoring atmosphere or generate new ones and the process is repeated. Accordingly, dislocation movement fluctuates between slow and fast motion and a serrated stress-strain curve results. At higher temperatures the solute mobility is such that there is little drag or interaction with the moving dislocation and a smooth stress-strain curve is again obtained. Since this process is diffusion controlled the magnitude and frequency of the serra-

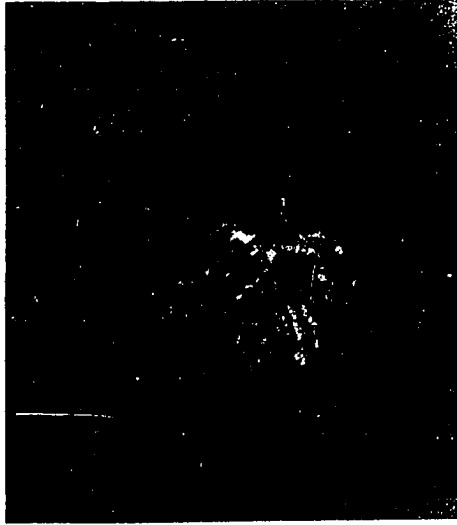


Figure 11. Example of a typical strained tensile specimen illustrating nearly 100% reduction in area X15

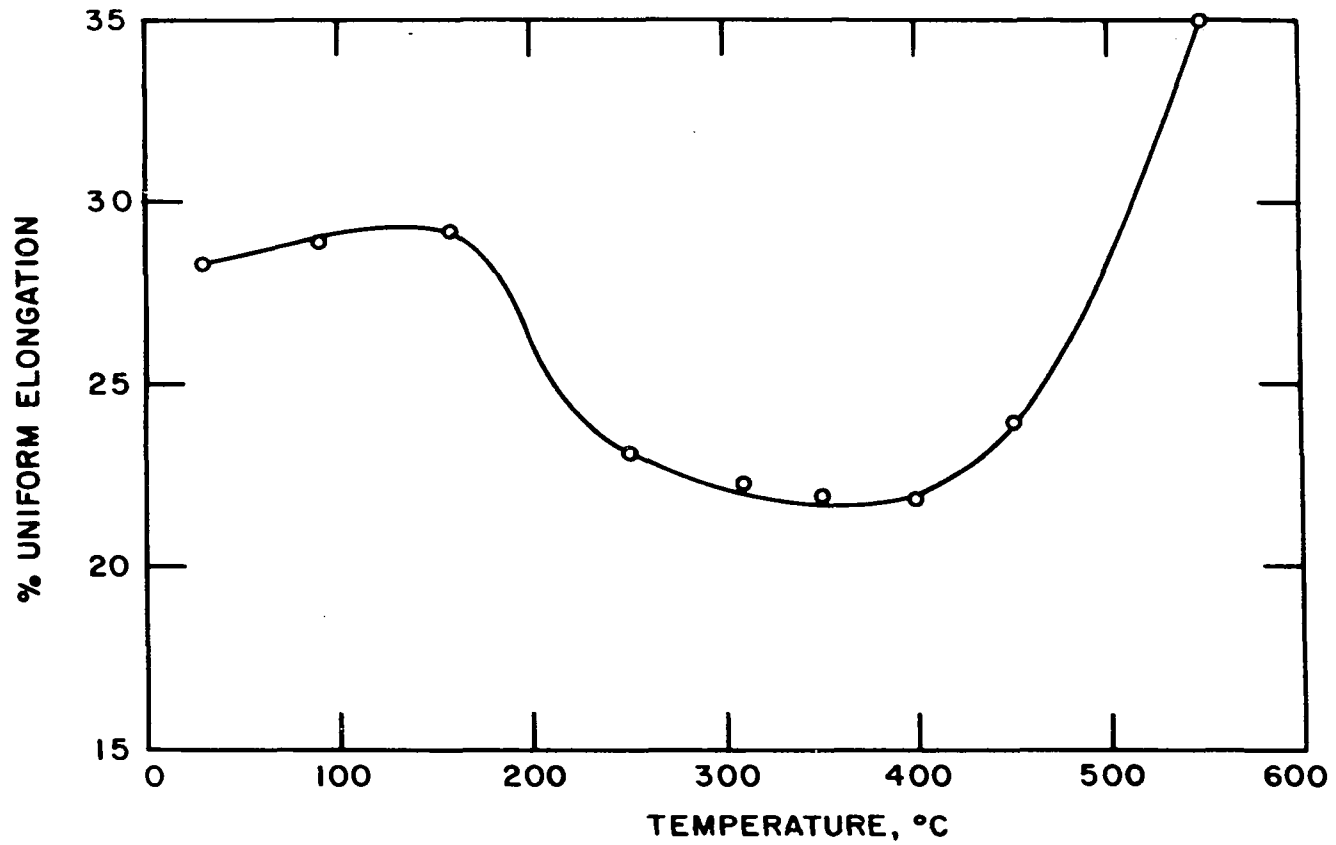


Figure 12. Effect of temperature on the uniform elongation of vanadium containing 120 ppm nitrogen

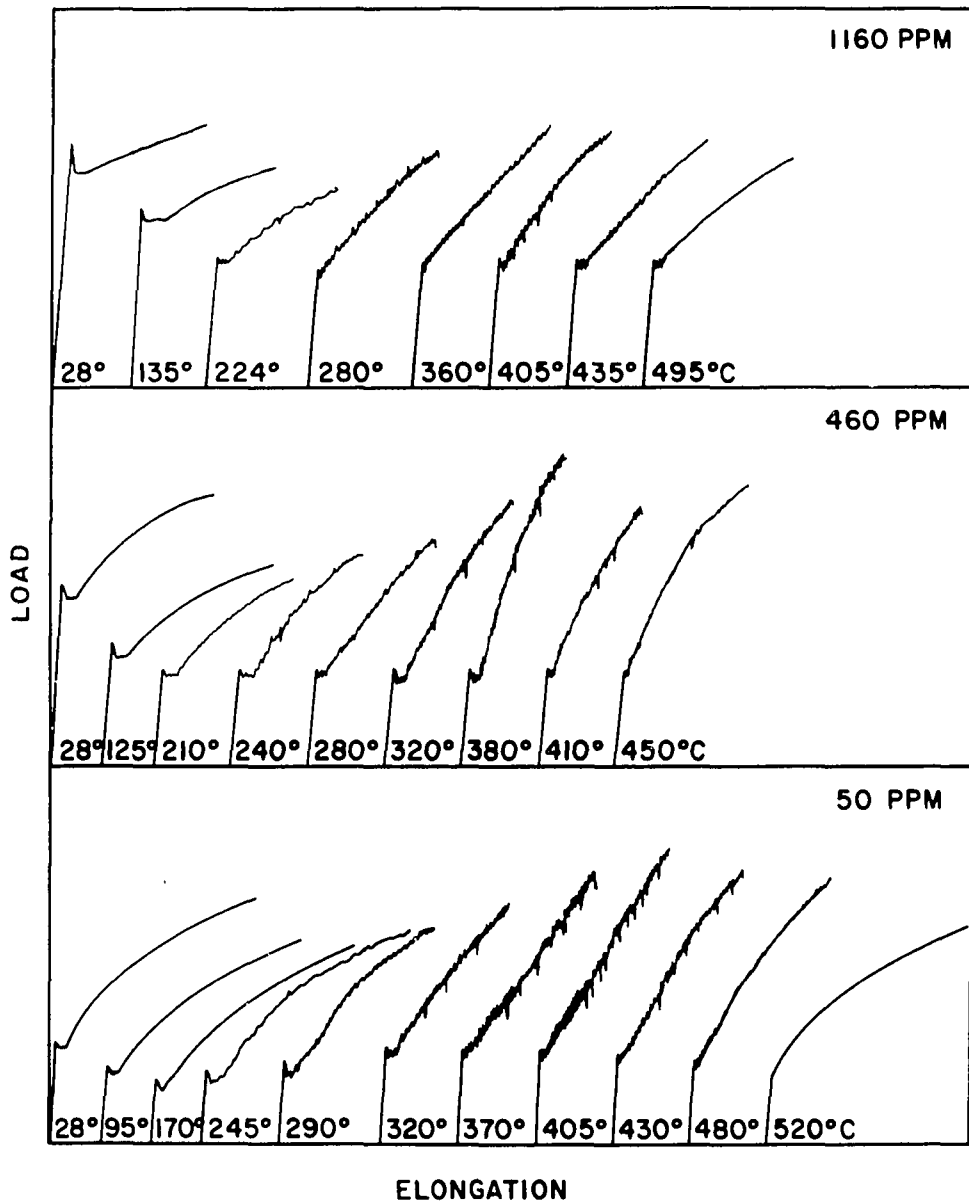


Figure 13. Typical flow curves illustrating the effect of temperature and nitrogen content on the occurrence of serrations

tions should depend upon the strain rate as seen from Fig. 14.

g. Activation energy      Of the preceding mechanical properties altered by the strain aging phenomenon the ultimate tensile strength could be reproduced with the greatest reliability and thus this parameter was used to calculate the activation energy associated with the strain aging peak. The strain aging peak was found to be strain rate sensitive, shifting to higher temperatures with increasing strain rates; hence an activation energy  $Q$  was determined from the conventional rate equation

$$\dot{\epsilon} = A \exp(-Q/RT)$$

where  $\dot{\epsilon}$  is the strain rate,  $A$  a constant,  $R$  the gas constant and  $T$  the strain aging peak temperature. From this equation it can be seen that a plot of  $\log \dot{\epsilon}$  versus  $1/T$  should result in a straight line with a slope of  $-Q/2.303 R$  from which  $Q$  can be determined. Plots of ultimate tensile strength versus temperature for vanadium containing 100 ppm nitrogen strained at three different strain rates are shown in Fig. 15 (curves a). It was shown in Fig. 6 that the temperature of the strain aging peak was relatively insensitive to nitrogen content and so similar plots for vanadium containing 550 ppm nitrogen for two other strain rates (Fig. 15 b) would be expected to lie on

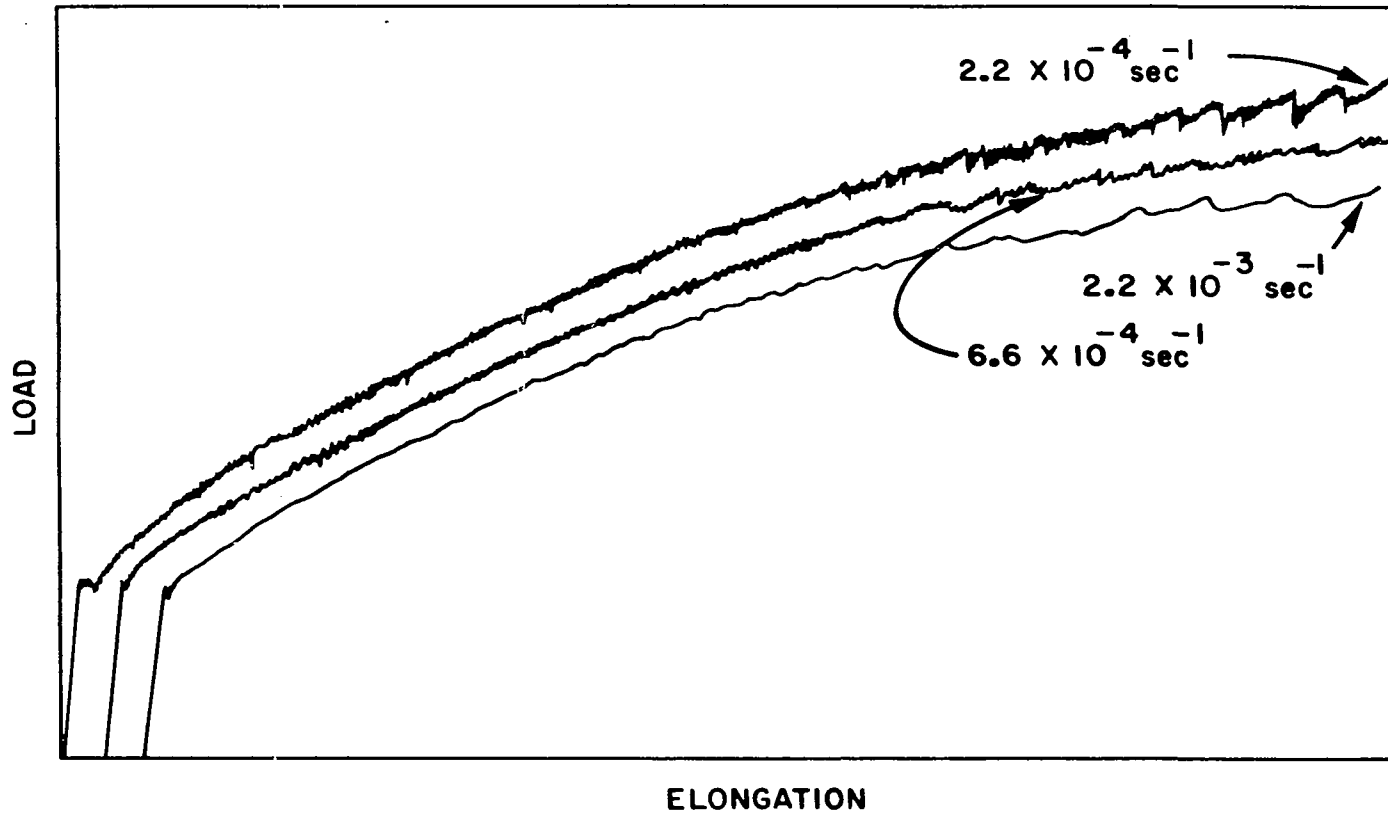


Figure 14. Typical flow curves illustrating the effect of strain rate on the occurrence of serrations in specimens containing 100 ppm nitrogen tested at 400°C

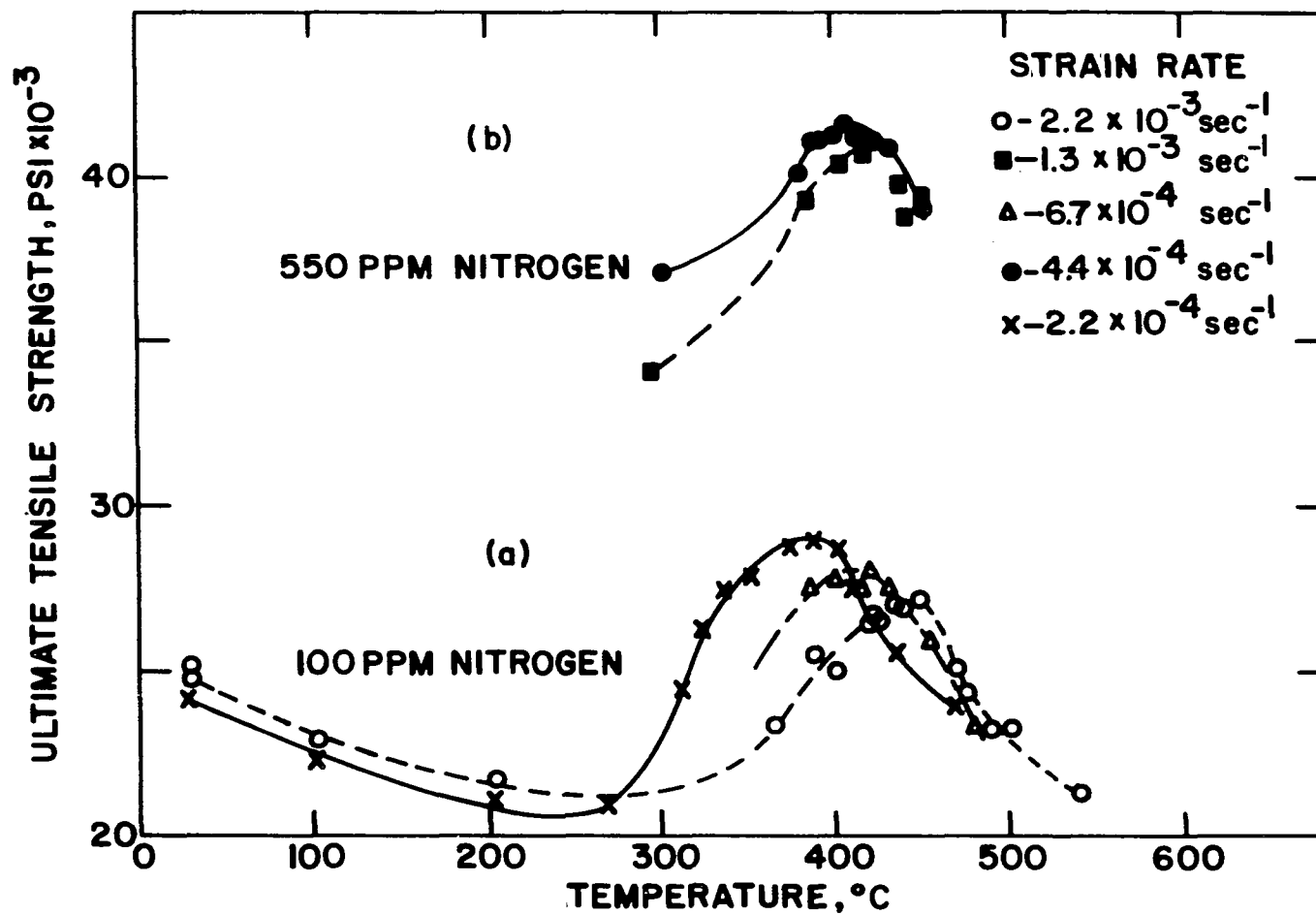


Figure 15. Effect of strain rate on the temperature of the strain-aging peak

the same  $\log \dot{\epsilon}$  versus  $1/T$  plot. This is indeed the case as can be seen from Fig. 16. The activation energy obtained from this method was calculated using a least squares treatment. A value of  $37.3 \pm 3.7$  kcal/mole was obtained.

The widely accepted mechanism of dynamic strain aging, which depends upon the interaction between interstitial atoms and dislocations, requires that the activation energy for the strengthening process be equal to the activation energy for the diffusion of the responsible atomic species. Values of the activation energy of the interstitials commonly present in vanadium are given in Table 4.

Table 4. Summary of activation energy data for interstitials in vanadium

Diffusing element	Q, kcal/mole	Reference
Nitrogen	$36.7 \pm 2.1$	76
	34.1	77
	34.6	78
	35.1	80
Oxygen	$27.9 \pm 0.9$	76
	28.6	77
	29.3	79
	29.6	78
	28.2	80
Carbon	27.3	79

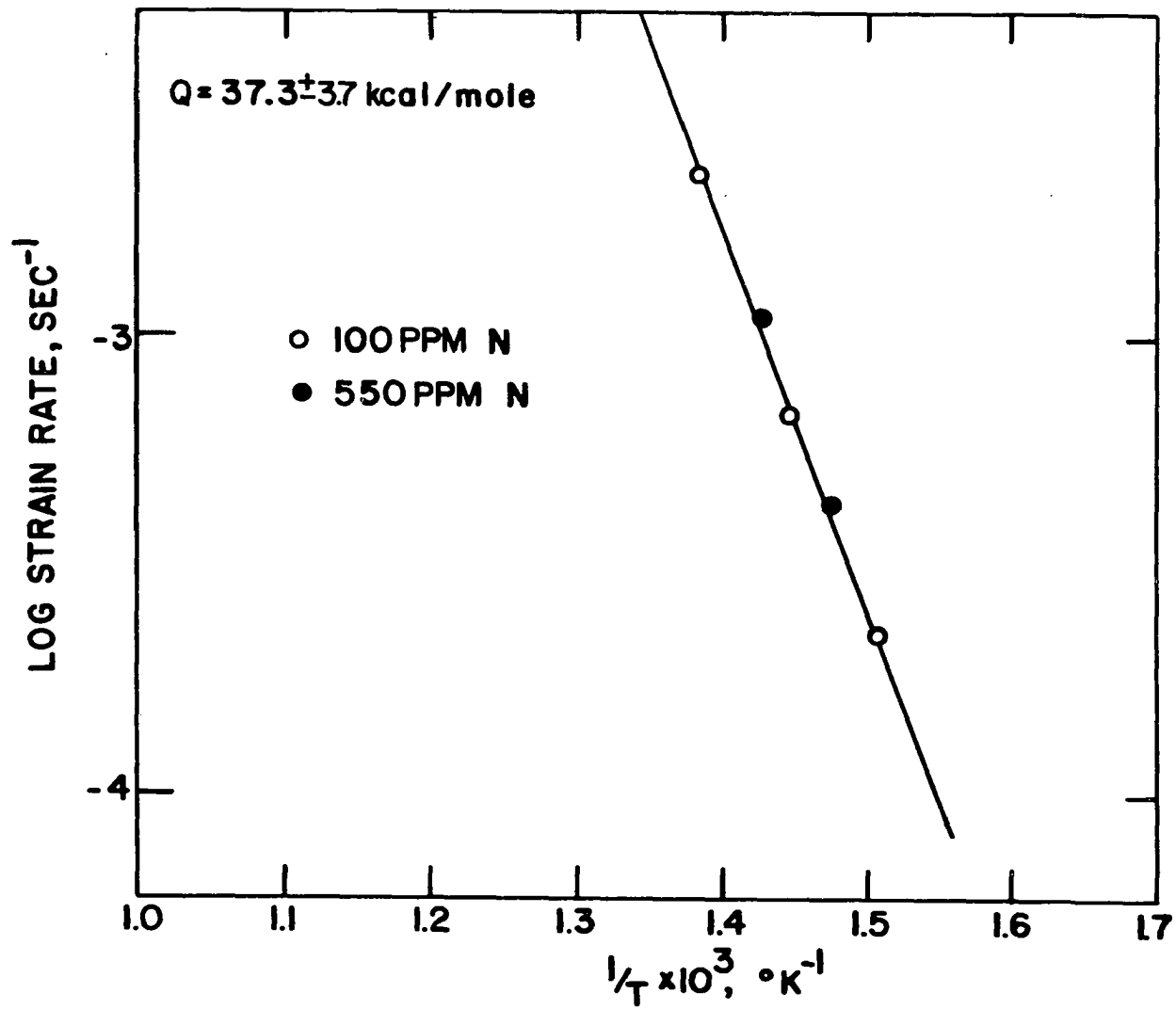


Figure 16. Arrhenius plot of the strain rate and strain-aging peak temperature

A comparison of the experimentally determined value with the data of Table 4 indicates that nitrogen is the solute responsible for the strain aging observed in these experiments.

h. Impact forming Keh and Leslie (74) noted that low carbon steel deformed at 200°C had a high work-hardening rate and contained a dislocation density an order of magnitude greater than a specimen deformed at room temperature. Vanadium also has a high rate of work hardening in the 300 to 500°C range. Therefore it was thought that it would be interesting to see if vanadium deformed in this temperature range but at a much higher rate would show evidence of this strengthening. Cylindrical billets prepared from vanadium containing 120 ppm nitrogen were impact extruded at various temperatures into 0.285 inch diameter rods. From a plot of the length of rod extruded versus extrusion temperature, Fig. 17, it can be seen that there is an apparent plateau in the 300 to 500°C range. Although no definite conclusions can be drawn from this test due to uncertainties in the actual specimen temperature and deformation rate it is interesting to note that this plateau corresponds fairly well with the relatively temperature independent region for the yield strength as shown in Fig. 8. Tensile specimens were then

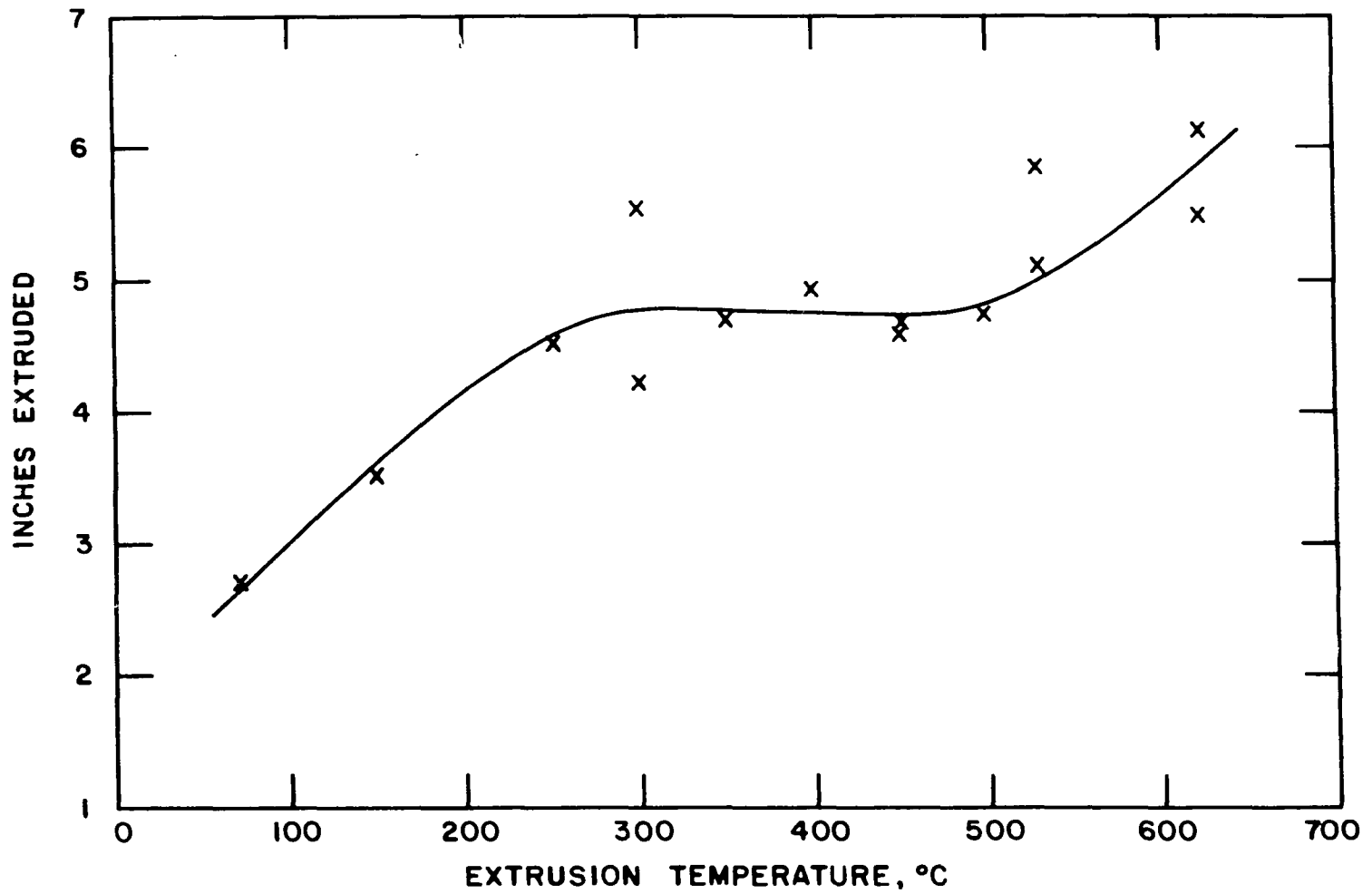


Figure 17. Influence of temperature on the length of extruded rod for vanadium containing 120 ppm nitrogen

machined from these rods and tested at room temperature in the as-extruded condition.

A continuous decrease in strength with increasing temperature was obtained from a plot of the room temperature tensile strength versus the extrusion temperature as shown in Fig. 18. This behavior suggests to the writer that at the high deformation rate employed in these tests there is insufficient time for strain aging to occur and therefore only the normal decrease in strength is observed. The strength of the extruded specimens was increased by about a factor of two over that in the recrystallized condition. These specimens deformed in a much smoother manner and terminated in a characteristic cup and cone type fracture as shown in Fig. 19. (Compare with Fig. 9.)

## 2. Static strain aging

Another parameter amenable to an activation energy analysis is the return-of-yield point. In order to investigate this effect a series of tests was performed at various temperatures in which specimens containing 600 ppm nitrogen were strained beyond the lower yield extension, unloaded and held under a small load to maintain sample alignment, aged at test temperature and reloaded. Tests were made to show that the

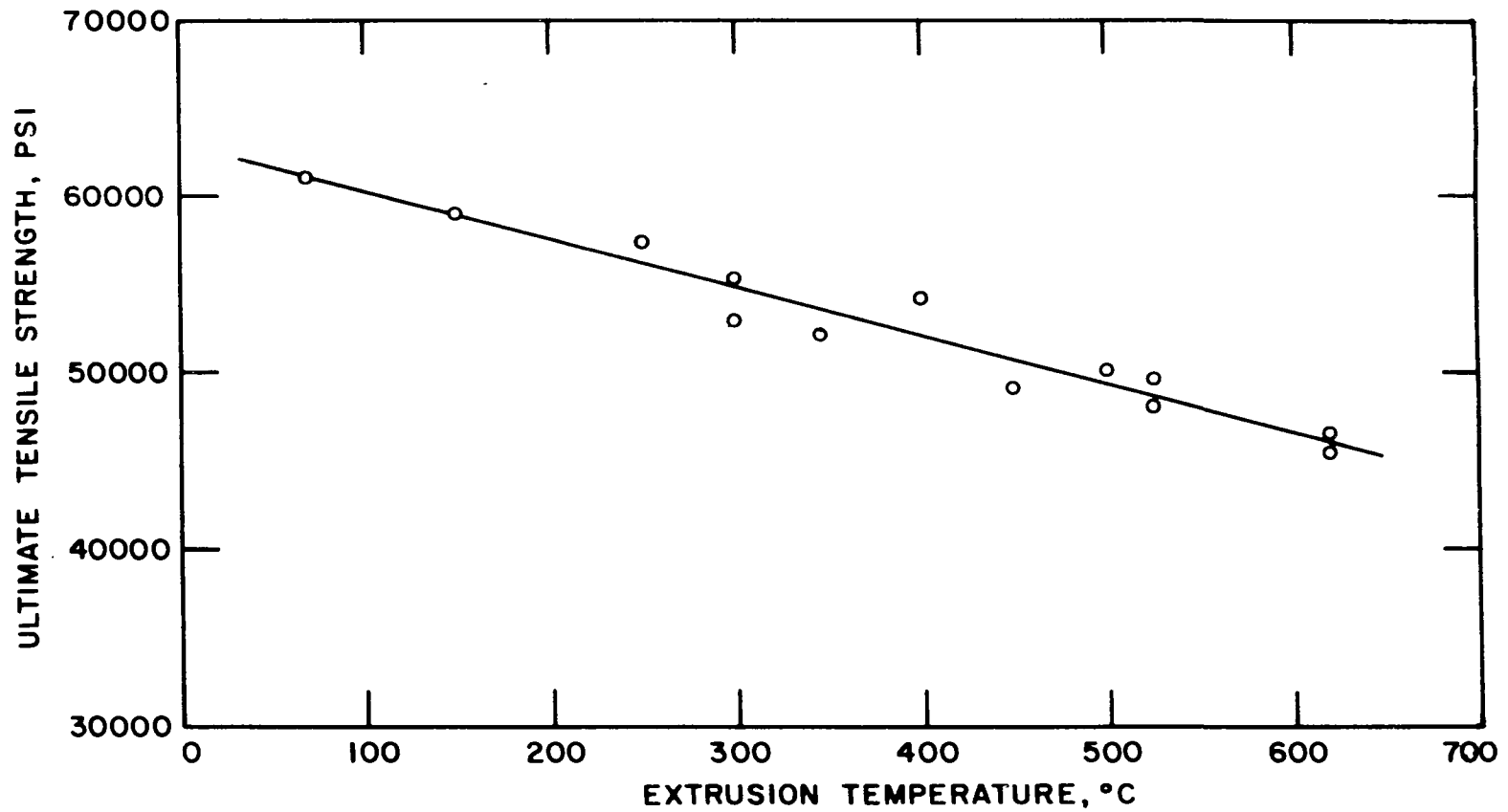


Figure 18. Effect of extrusion temperature on the room temperature tensile strength of as-extruded specimens



Figure 19. Example of a typical tensile specimen tested in the as-extruded condition X15

magnitude of the yield point was unaffected by the preceding tests provided the specimen was strained beyond the lower yield extension. Therefore several tests with intermittent treatments were run on each specimen as is illustrated in Fig. 20.

According to the Cottrell-Bilby equation a plot of the fraction of solute atoms segregated to the dislocation versus  $t^{2/3}$  should result in a straight line. Following the assumption of Bolling (81) that  $\Delta\sigma/\sigma$  (see Fig. 20) is proportional to the amount of solute diffusing to the dislocation, where  $\sigma$  is the flow stress and  $\Delta\sigma$  the increase in flow stress due to strain aging, plots of  $\Delta\sigma/\sigma$  versus  $t^{2/3}$  for six aging temperatures are shown in Fig. 21. The temperature dependence of the rate of yield-point return for this material was found to be adequately expressed by an empirical rate equation of the form:

$$1/t = A \exp(-Q/RT).$$

Assuming that equal values of  $\Delta\sigma/\sigma$  represent conditions for equivalent amounts of solute to segregate to dislocations, Fig. 22 may be plotted for an arbitrary mean value of 0.02 from the data of Fig. 21. The activation energy determined from the slope of this curve, using a least squares analysis,

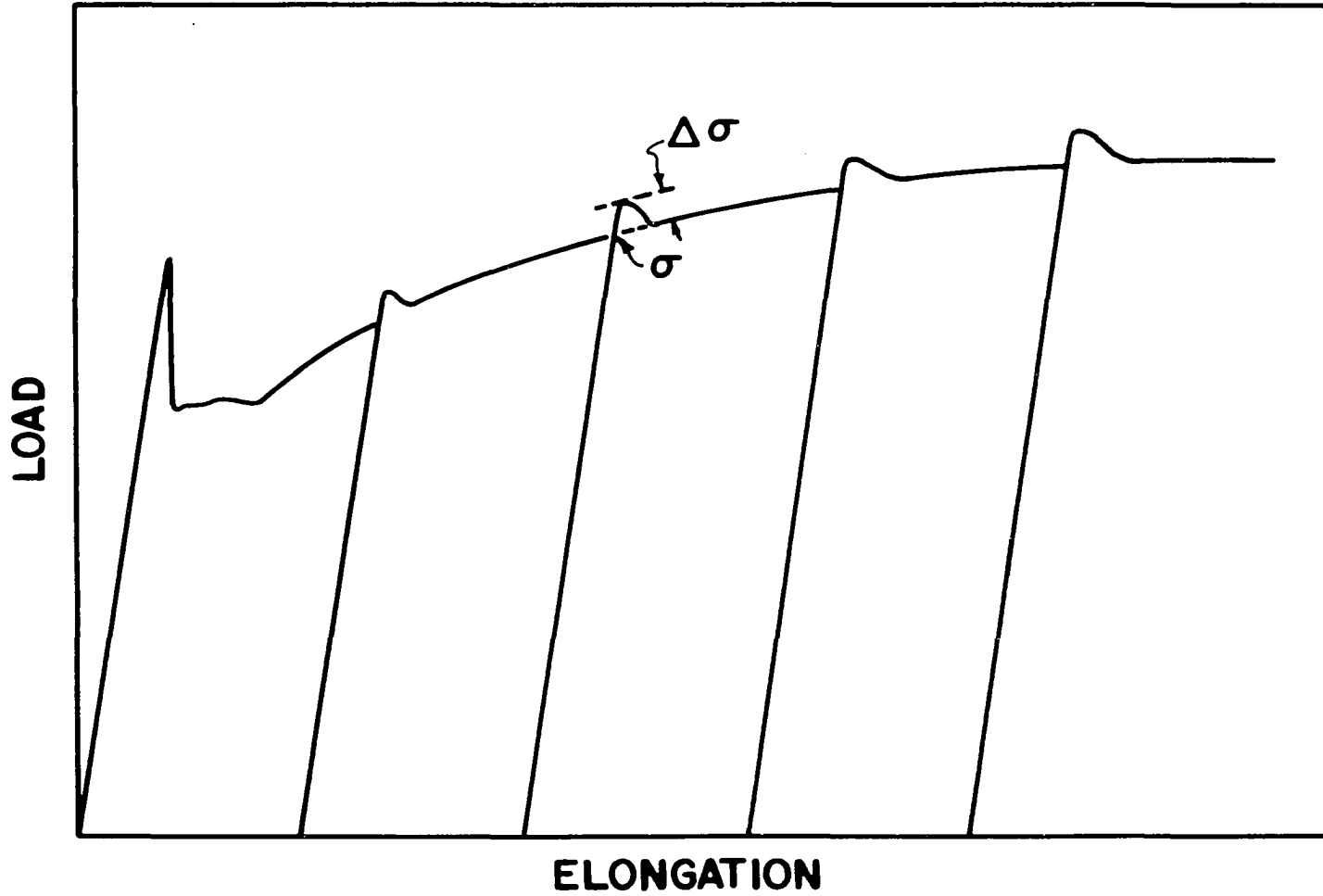


Figure 20. Schematic load-elongation curves illustrating the yield point return upon aging

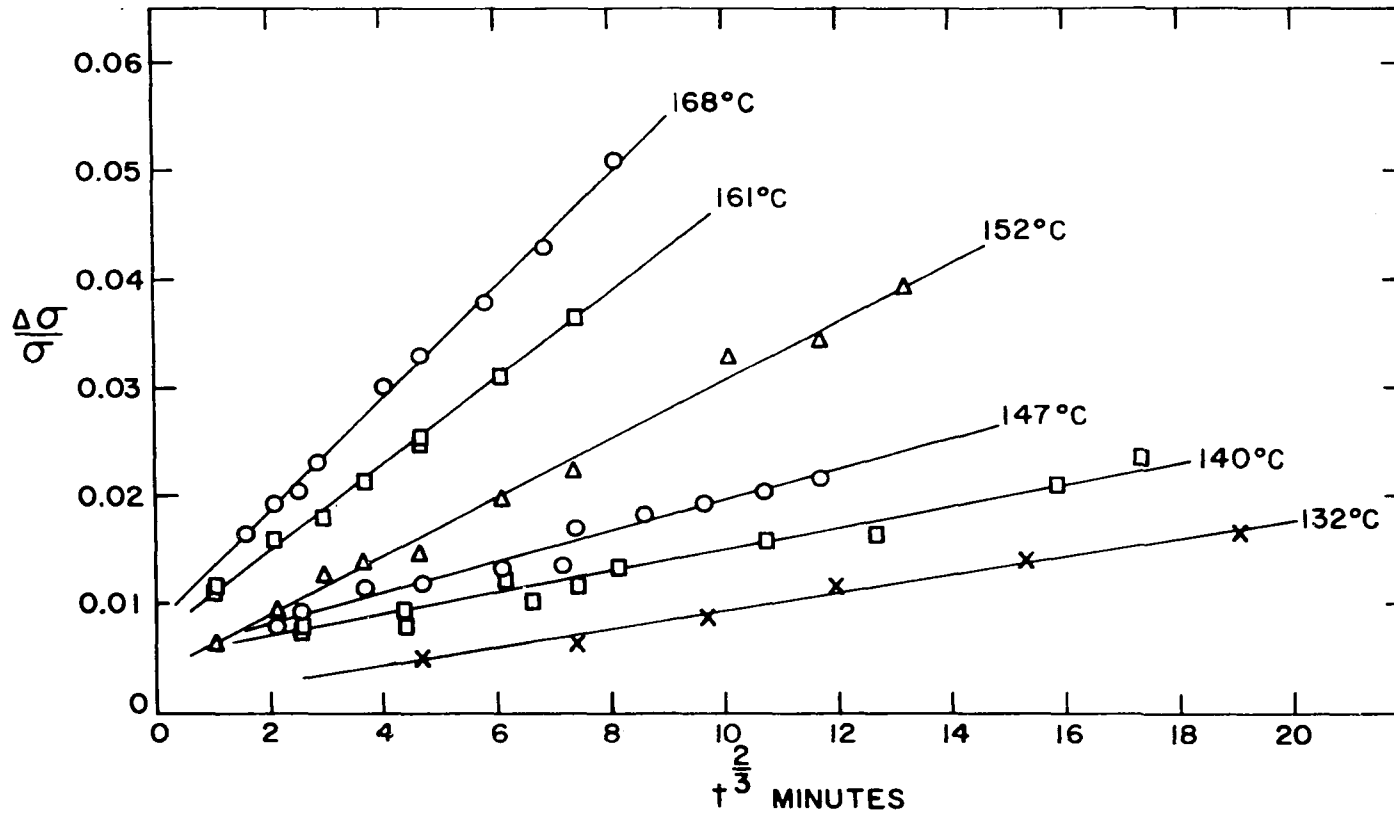


Figure 21. Plots of relative hardening against aging time for different aging temperatures

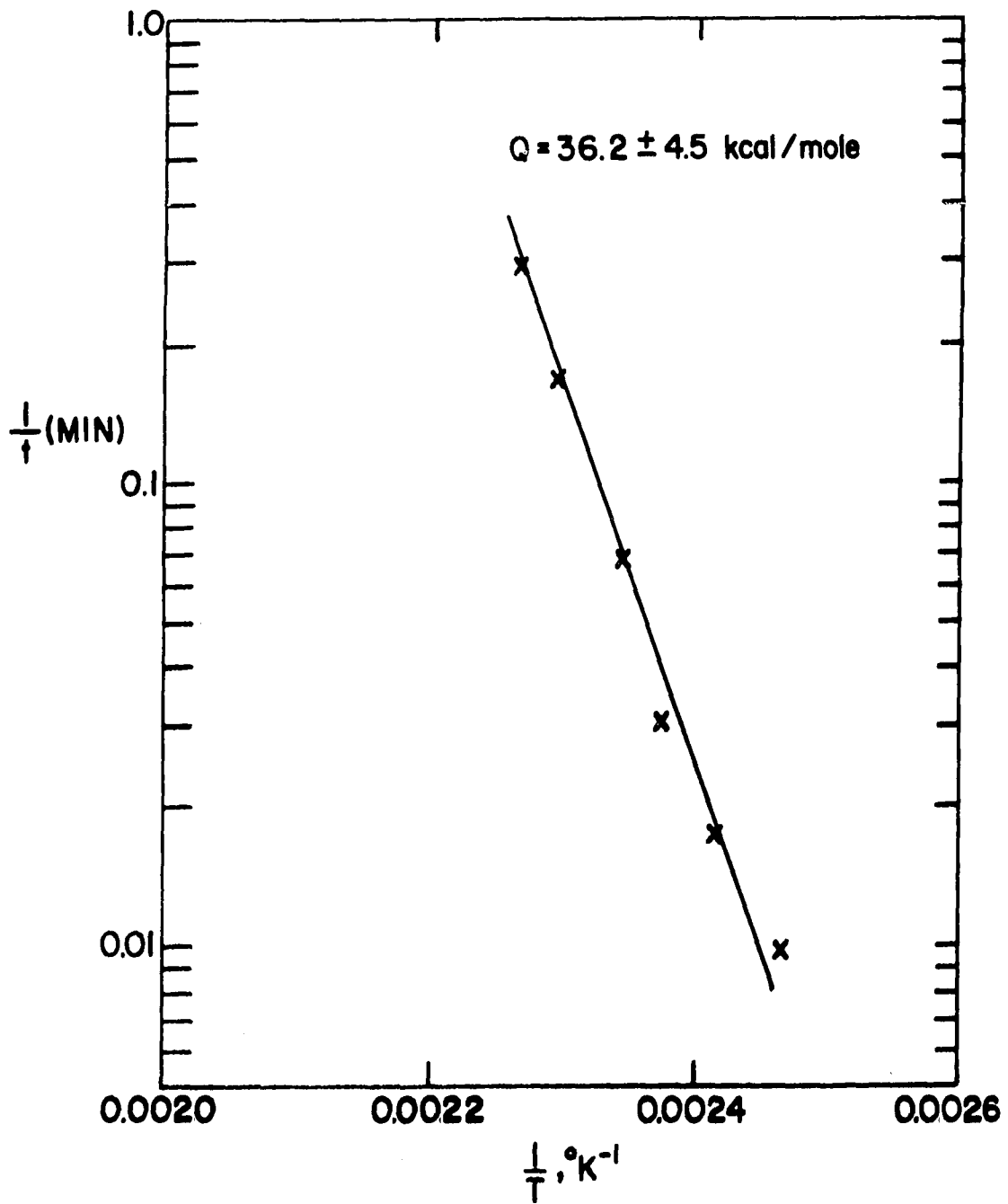


Figure 22. Plots of reciprocal of time to attain equivalent amount of strain aging versus reciprocal aging temperature for data taken from Figure 21

was  $36.2 \pm 4.5$  kcal/mole. This value is in good agreement with that obtained by the dynamic method described above and with the activation energy for diffusion of nitrogen in vanadium as reported in the literature.

Bradford and Carlson (44) working with vanadium containing 265 ppm oxygen, 150 ppm carbon and  $<5$  ppm nitrogen obtained an activation energy of 27.7 kcal/mole using a return-of-yield point method. They attributed the yield point to oxygen or carbon since both elements have activation energies for diffusion in vanadium very close to this value. Because of the evidence presented above for a nitrogen-induced yield point, static strain aging tests on vanadium containing 170 ppm oxygen, 150 ppm carbon and 30 ppm nitrogen were run in an effort to verify or refute these earlier results. An activation energy of 27.1 kcal/mole was obtained from these tests which is in agreement with Bradford's value. From these data one concludes that oxygen (or possibly carbon) produces a yield point in vanadium when present in sufficient quantities and when it is not masked by the stronger nitrogen effect. Obviously it would be interesting to study this phenomenon in vanadium of higher purity than was available for this investigation.

No evidence of strain age hardening was found in this investigation. On straining beyond the yield point, the flow curve returned to the curve obtained by extrapolation of the data prior to aging, thus indicating that the hardening resulting from the strain aging was transient. This transient nature of strain aging is further illustrated by Fig. 23 which shows the flow curve for a specimen continuously deformed at 152°C and for a specimen deformed and aged at this same temperature. Within experimental error the two flow curves are identical indicating that repeated aging has no effect on the flow curve, at least in this temperature range.

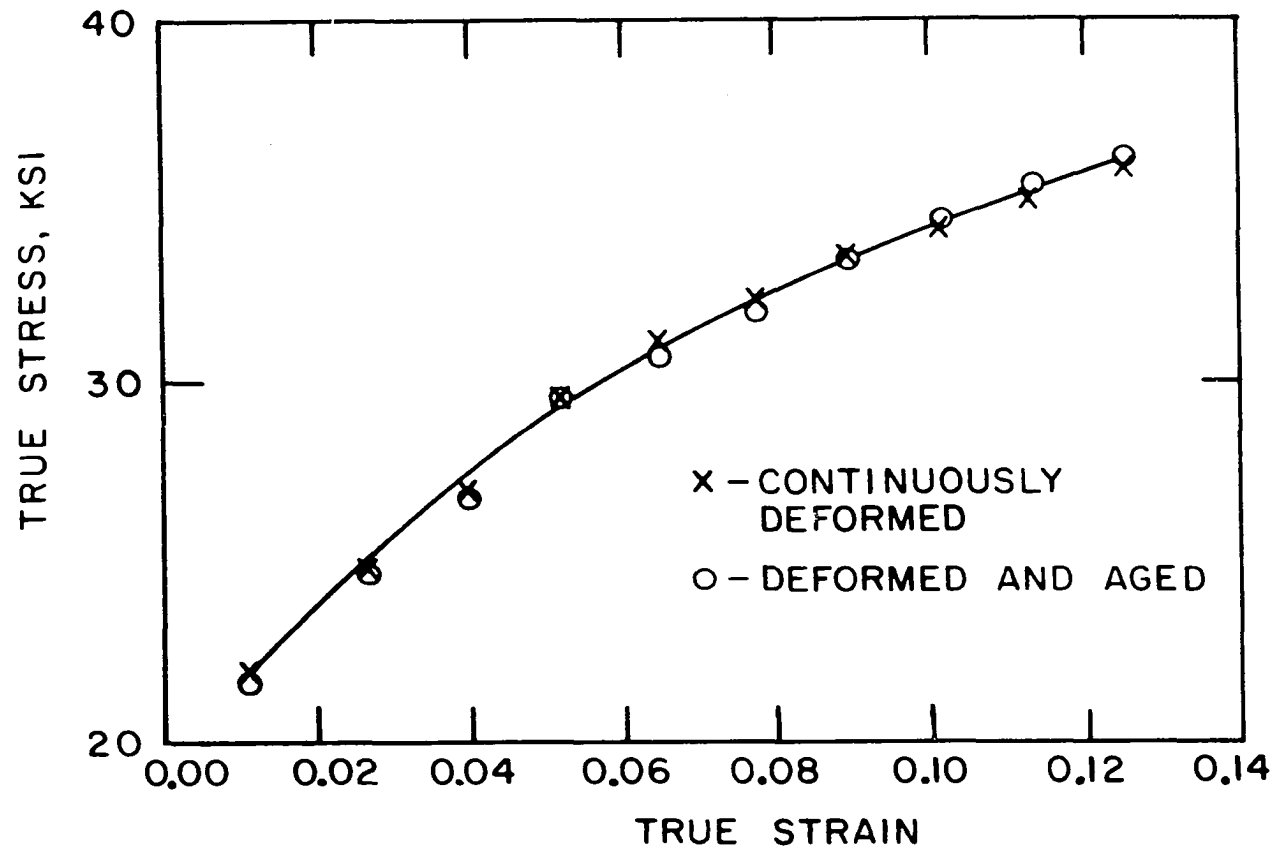


Figure 23. Flow curves at 152°C for one specimen continuously deformed and another alternately deformed and aged illustrating the transient nature of hardening due to strain aging

## B. Brittle-Ductile Transition

Most of the refractory metals undergo a ductile-to-brittle transition characterized by a pronounced drop in ductility with decreasing temperature over a narrow temperature range, the mode of fracture at the higher temperatures being of the shear type while the lower temperatures promote cleavage fracture. In the case of iodide-refined vanadium, however, no brittle-ductile transition is observed down to liquid nitrogen temperatures. Hence it was decided to investigate the effects of separate additions of nitrogen and carbon on the ductility of iodide-refined vanadium, the additions being kept under 6000 ppm, in which case nitrogen was in solid solution while carbon formed a dispersed second phase in nearly all alloys. To evaluate this property bend tests were performed in three-point bending from room temperature down to  $-196^{\circ}\text{C}$ . The specimens were classified as ductile if they underwent a deflection of 0.250 inch without cracking, which was approximately a  $90^{\circ}$  bend and brittle if cracks appeared before this deflection was reached. In almost all cases however, brittle specimens fractured at very small deflections and hence there was no difficulty in determining the onset of brittleness.

## 1. Effect of nitrogen

a. Polycrystalline samples      The hardness of vanadium is quite sensitive to the amount of dissolved nitrogen and, provided that no oxygen contamination occurs, hardness can be used as a measure of the nitrogen content. The relationship between nitrogen content and the diamond pyramid hardness of recrystallized vanadium is shown in Fig. 24.

Although the strength and hardness increase markedly with nitrogen content no brittle fracture was observed down to  $-196^{\circ}\text{C}$  for specimens containing less than 2000 ppm nitrogen. Above this concentration the alloys are quite hard requiring considerable care in the fabrication of the specimens. A plot of the transition temperature as a function of nitrogen content is shown in Fig. 25 where it is seen that the transition temperature increases with increasing nitrogen content.

After extensive examination of many specimens it was concluded that fracture was initiated at grain boundaries and propagated transgranularly although in some cases a small amount of accommodation fracture at the grain boundaries linking cracks in adjacent grains was found. Examples of the microstructure of the fracture surface in a typical brittle specimen are shown in Fig. 26. Many small cracks were

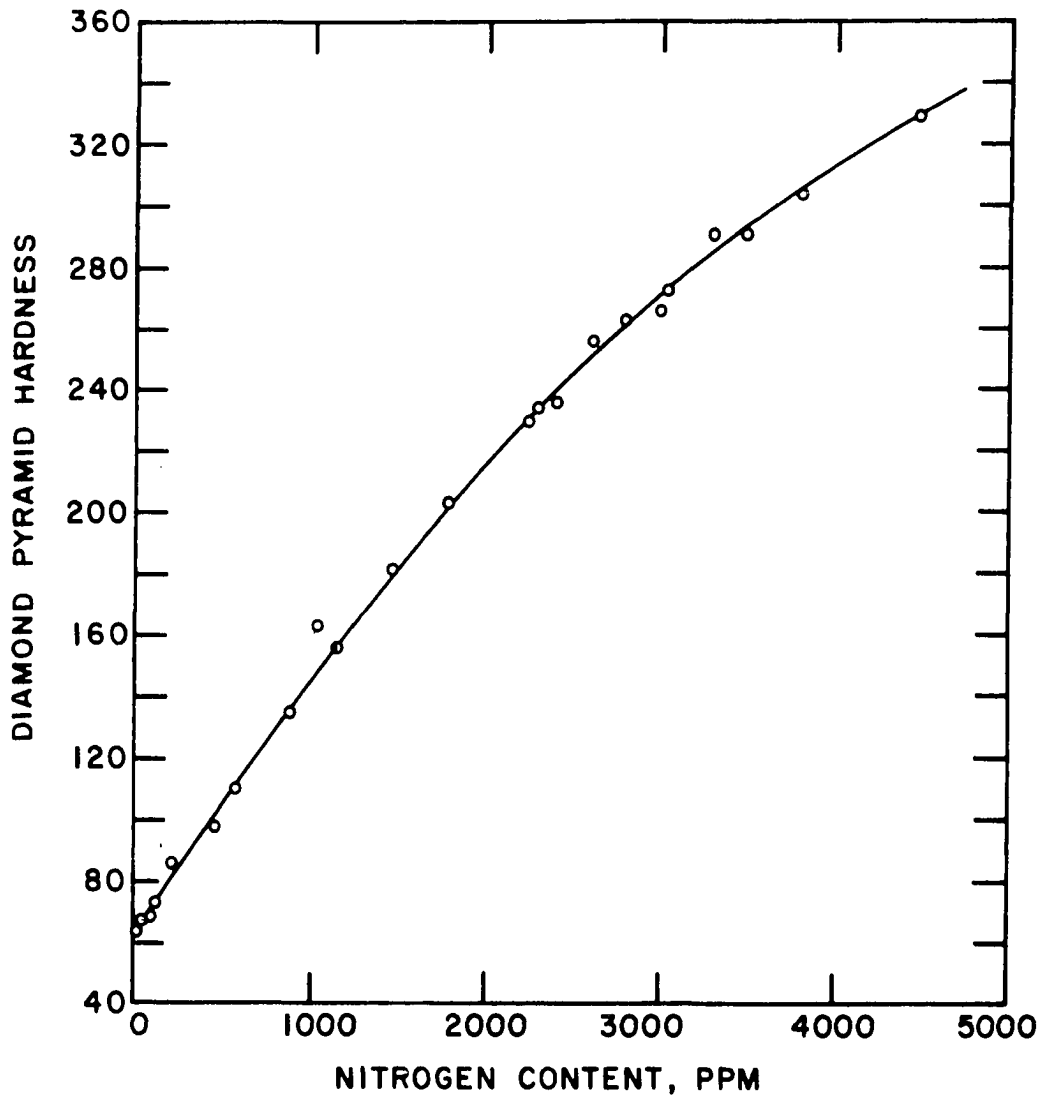


Figure 24. Effect of nitrogen on the hardness of vanadium

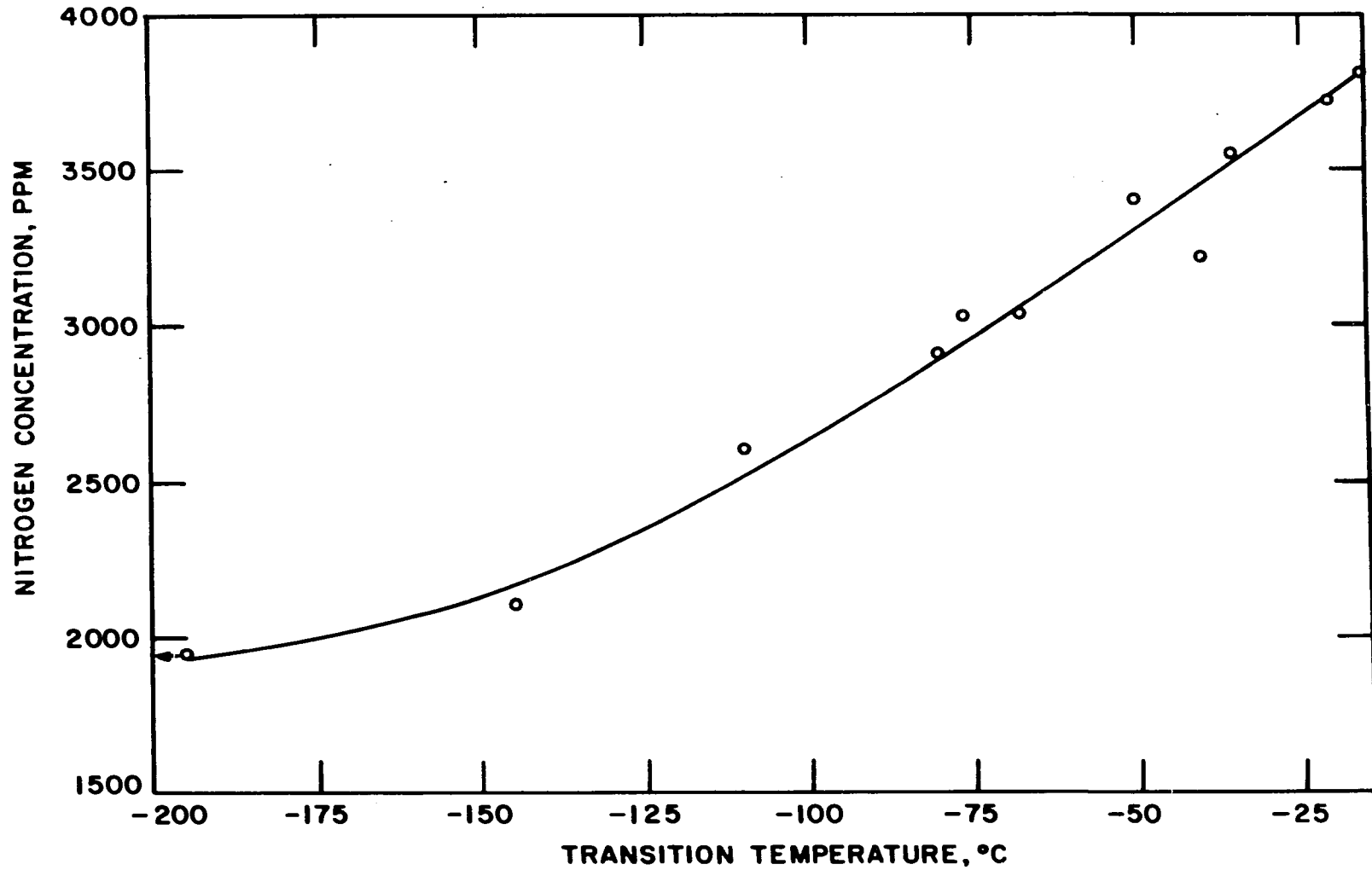


Figure 25. Effect of nitrogen on the brittle-ductile transition of polycrystalline vanadium

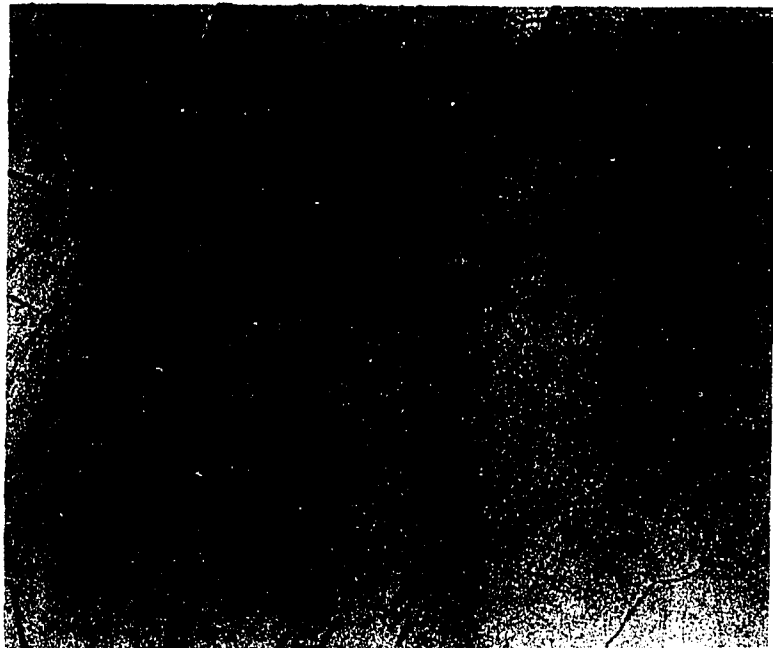
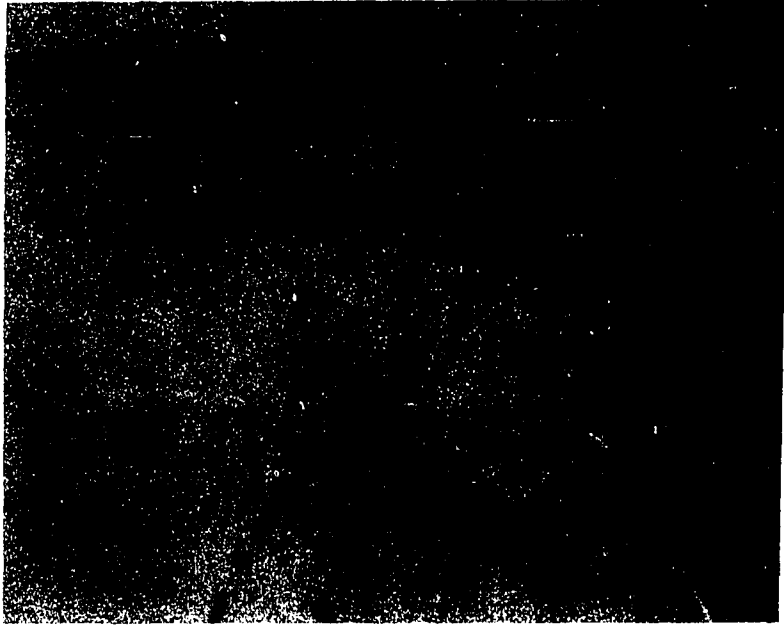


Figure 26. Examples of crack nucleation at grain boundaries X100

observed in a single specimen indicating that in the polycrystalline case crack propagation is the controlling factor. Carbon replicas of these specimens were also prepared and examined with an electron microscope for evidence of grain boundary precipitates, but none were found thus eliminating the possibility that cracks are initiated at second phase particles in these alloys.

b. Monocrystalline samples From metallographic examination of the fractured polycrystalline specimens it was concluded that grain boundaries play an important role in the brittle-ductile transition of vanadium-nitrogen alloys. To investigate this dependency a series of monocrystalline samples of various nitrogen concentrations were prepared by arc-zone melting and the resulting specimens were tested under conditions identical to those employed for the polycrystalline specimens. The data are plotted in Fig. 27 which gives a curve of the same shape as that for the polycrystals but displaced 50 to 60°C lower for equivalent nitrogen concentrations. Microscopic examination of the fractured specimens indicated that failure had occurred by propagation of a single crack across the entire specimen since no small isolated

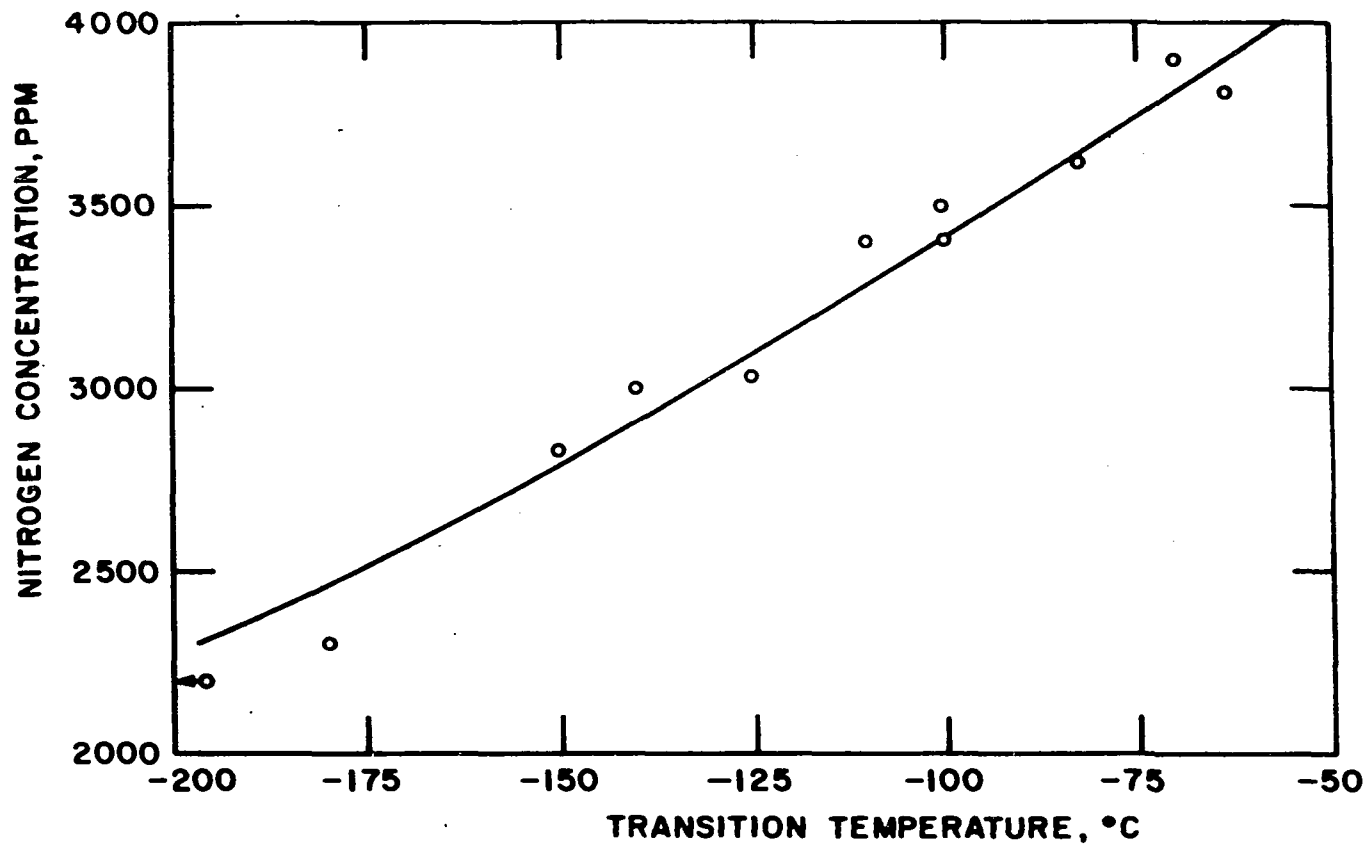


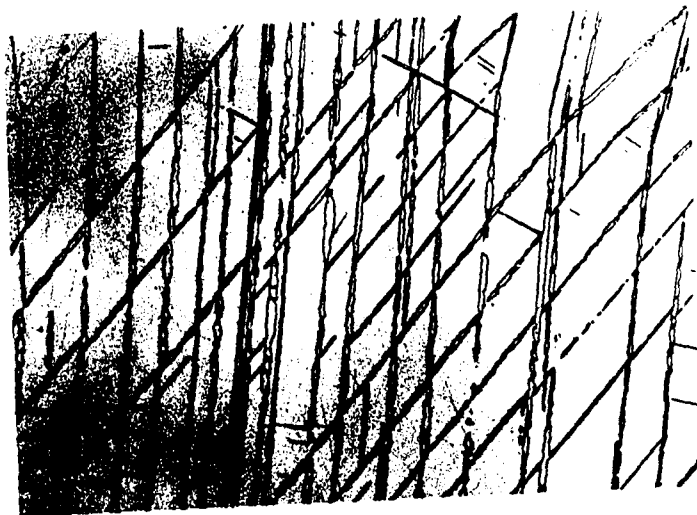
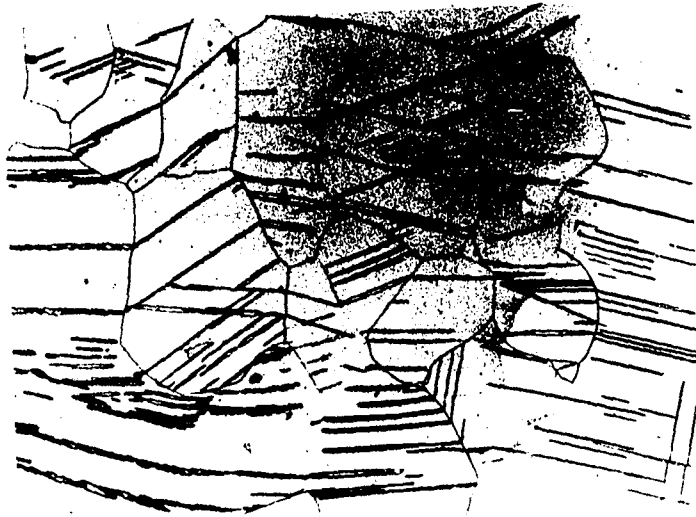
Figure 27. Effect of nitrogen on the brittle-ductile transition of monocrystalline vanadium

cracks, as were found in the polycrystalline specimens, were visible. These results indicate that for the monocrystalline case crack nucleation is the predominant factor in brittle failure of vanadium-nitrogen alloys in contrast to the polycrystalline case in which crack propagation appears to be the controlling factor. No conclusive evidence for crack nucleation sites was obtained although the possibility of their initiation at twin boundaries was investigated and is described in the next section.

c. Mechanical twinning Mechanical twinning was observed in iodide-refined vanadium and in all vanadium-nitrogen alloys tested. However, as would be expected, a temperature dependency for the onset of twinning was noted and no twinning was observed in specimens tested above  $-90^{\circ}\text{C}$ . Twins observed at  $-90^{\circ}\text{C}$  were only present in or immediately adjacent to grains which had cleaved and it was necessary to decrease the test temperature to  $-110^{\circ}\text{C}$  before twins were present in grains removed from the immediate fracture area or in ductile specimens. Although Clough and Pavlovic (51) reported twins to be present in layers of only one or two grains in thickness immediately adjacent to cleaved surfaces in commercially pure vanadium, in this investigation twinning

was observed in both brittle alloy specimens and in ductile, high-purity vanadium. These data indicate that twinning is suppressed in the commercially pure vanadium probably due to stress relaxation around precipitates. One interesting feature to be noted is that specimens tested at  $-140^{\circ}\text{C}$ , whether in the ductile or brittle condition exhibited a great profusion of twins in their microstructure, much more so than at other temperatures. An example of this profuse twinning is shown in Fig. 28a. The formation of twins at the intersection of twins with grain boundaries is shown in Fig. 28b and examples of the intersection of twins are shown in Fig. 28c. Although the coincidence may be entirely fortuitous, a minimum in ductility in hydrogen-embrittled vanadium (43) and an inflection in the brittle-ductile transition temperature of vanadium as a function of oxygen content (44) also occur in this approximate temperature region. Since twinning is reported to be associated with cleavage or brittle fracture in niobium (82) metallographic examination of the alloys tested was undertaken to determine whether or not twinning was associated with fracture nucleation. Although the results were inconclusive, and in general fracture initiation could not be traced to twinning, some apparent crack nuclei were found at

Figure 28. Photomicrographs of vanadium illustrating:  
(a) profuse twinning  
(b) twin nucleation at grain boundaries  
(c) twin intersections  
X100



twins as illustrated in Fig. 29.

## 2. Effect of carbon

a. Polycrystalline samples      Small quantities of carbon markedly increase the hardness and strength of vanadium with additional amounts having little if any further effect upon these properties. These results are shown in Figs. 30 and 31. The maximum bending load was calculated by dividing the total load on the specimen by its original cross-sectional area. The beginning of the plateaus in both cases corresponds to the estimated solubility limit of carbon in vanadium. This is supported by metallographic evidence as is described below.

Bend tests were performed between room temperature and  $-196^{\circ}\text{C}$  on a series of vanadium-carbon specimens. A plot of the yield load versus reciprocal temperature (Fig. 32) shows that the specimens containing 350 ppm carbon are appreciably stronger than the specimens containing 150 ppm and the specimens containing 3400 ppm carbon fall approximately half way between these two curves. These results are interpreted in the following manner. The 350 ppm specimens are stronger than the lower carbon specimens because of an increase in the amount of carbon in solid solution, dispersion hardening or both. The 3400 ppm specimens contained a considerable amount

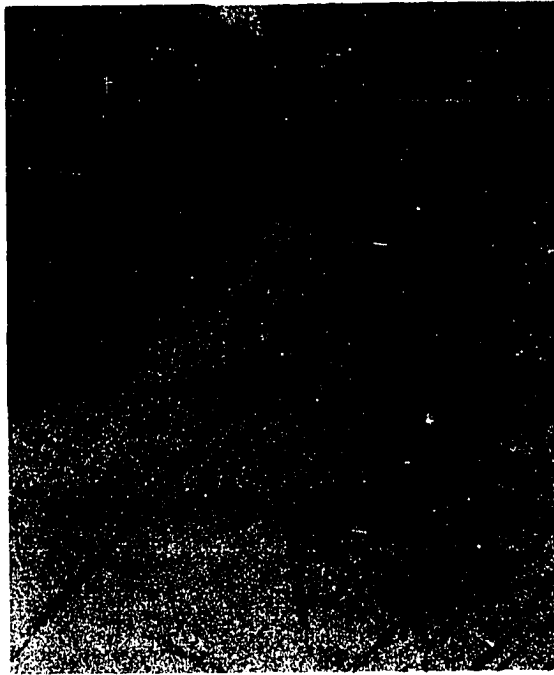


Figure 29. Examples of cracks nucleating at twins in vanadium X100

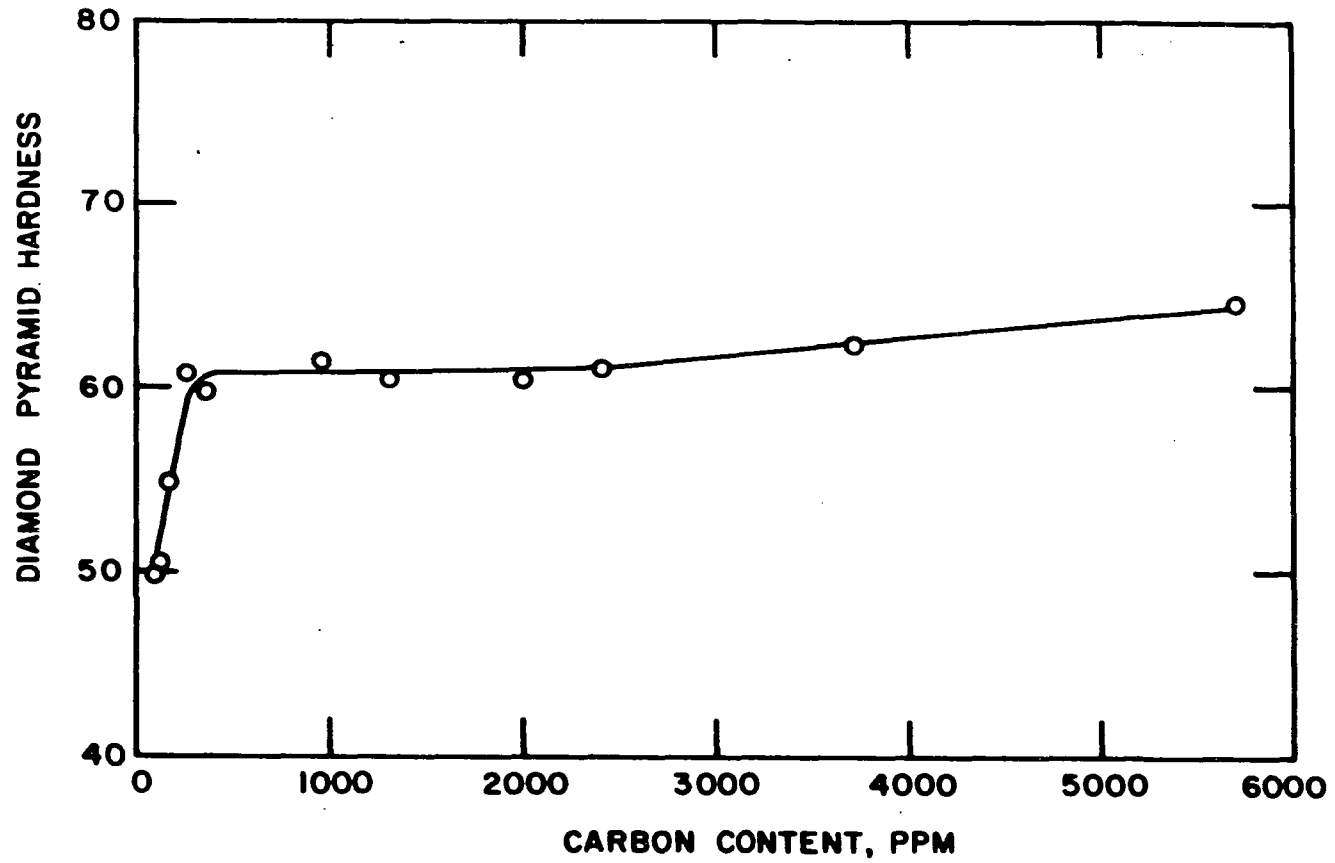


Figure 30. Effect of carbon on the hardness of vanadium

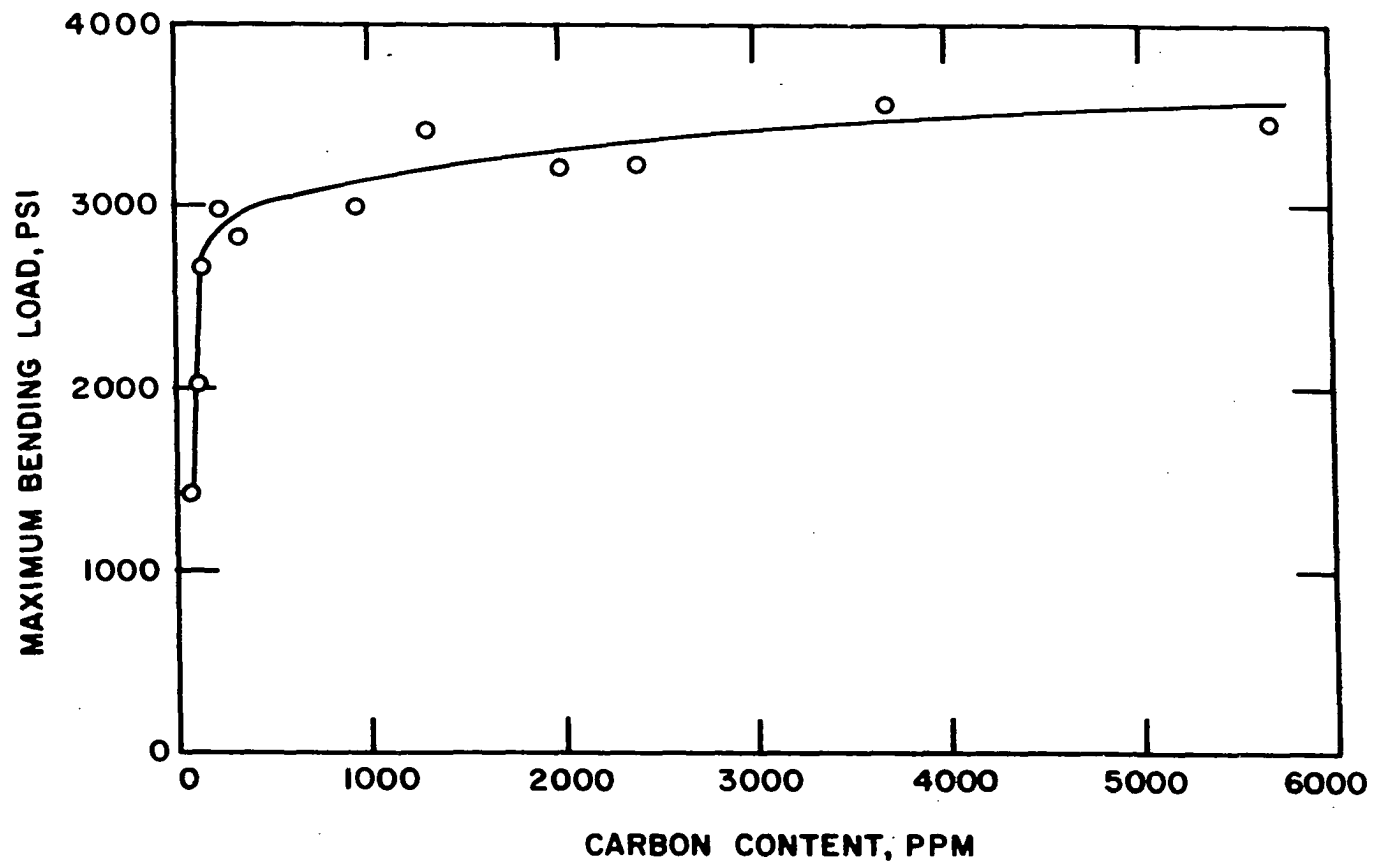


Figure 31. Effect of carbon on the maximum bending load in vanadium

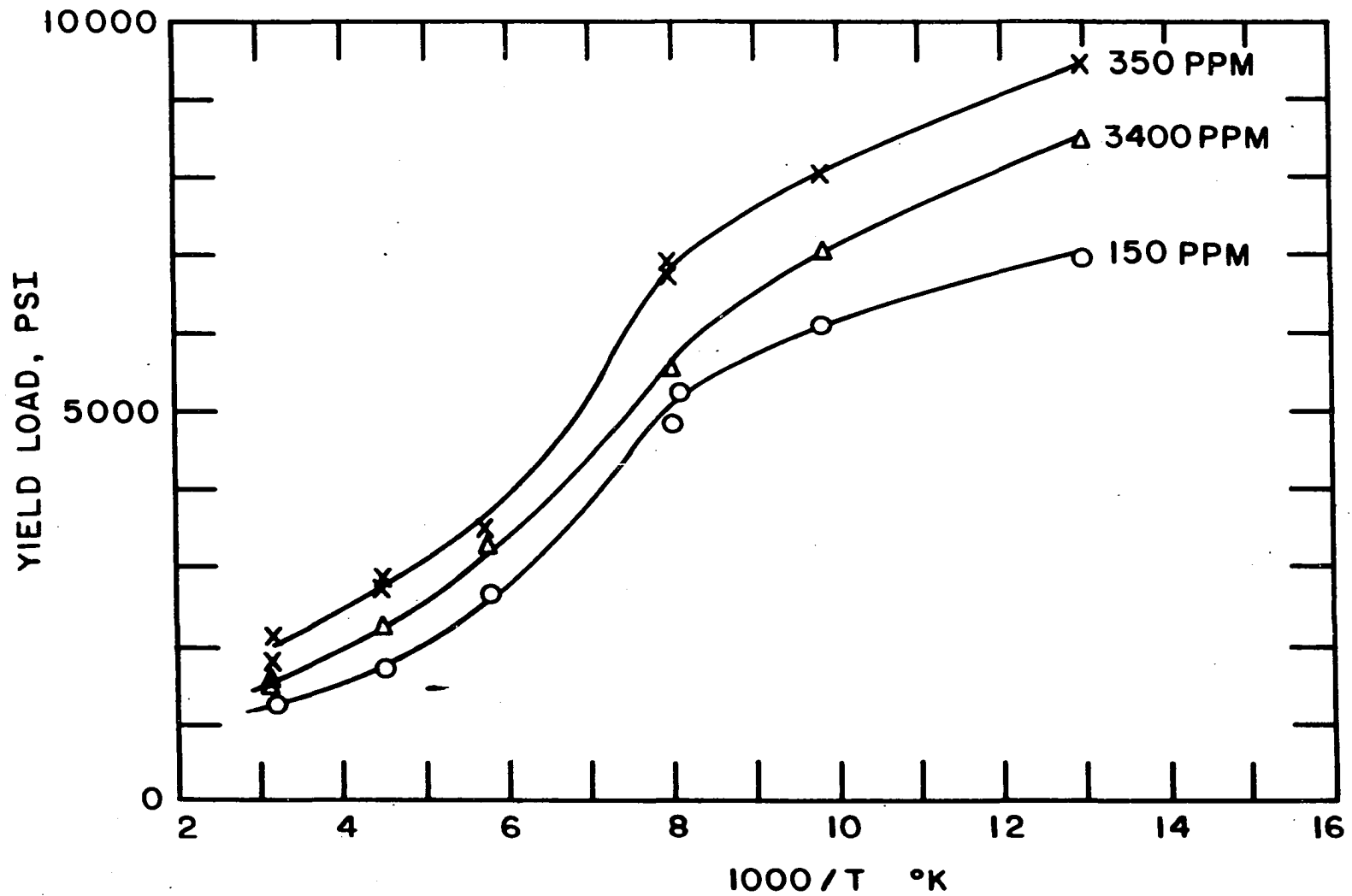


Figure 32. Effect of temperature and carbon on the yield load in bending

of second phase particles which inhibited recrystallization and during prolonged heat treatment these particles agglomerated and became less effective in strengthening the matrix. These data indicate, then, that the strengthening of the 350 ppm specimens is a result of both solid solution strengthening and the presence of a finely dispersed precipitate while the 3400 ppm specimen is lower in strength because its precipitates have been agglomerated by annealing. The photomicrographs in Fig. 33 support this conclusion.

No evidence was found, however, that the carbide dispersion had any appreciable effect on the embrittlement of vanadium since no cleavage fracture was observed for specimens containing up to 5700 ppm carbon and tested at  $-196^{\circ}\text{C}$ . However, in alloys containing 3400, 4500 and 5700 ppm carbon, cracks were observed along the semicontinuous carbide network segregated at the grain boundaries in specimens tested at  $-196^{\circ}\text{C}$ . These were not shiny, transgranular cleavage fractures like those found for the case of nitrogen embrittlement but were of the fibrous, intergranular, ductile type, examples of which are shown in Fig. 34.

b. Mechanical twinning Unlike the vanadium-nitrogen alloys, twinning was observed only in a few of the vanadium-

Figure 33. Photomicrographs of vanadium containing:  
(a) 150 ppm carbon  
(b) 350 ppm carbon  
(c) 3400 ppm carbon  
X100

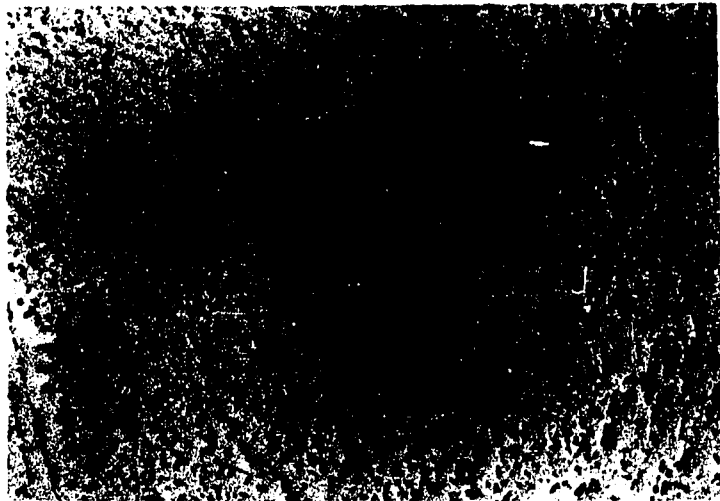
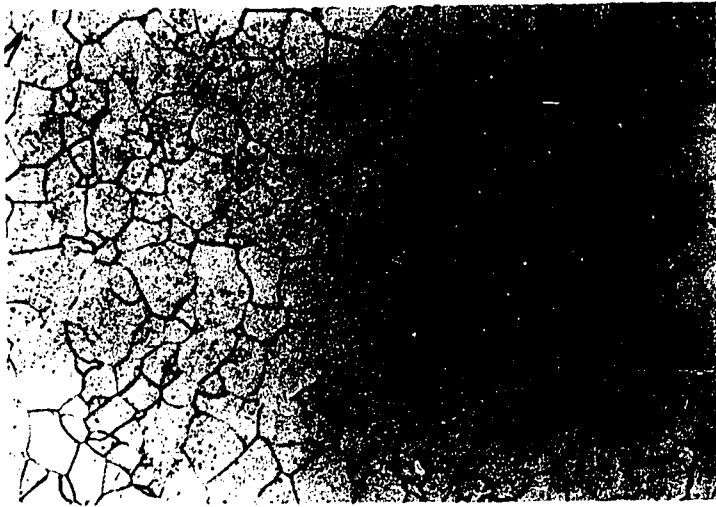
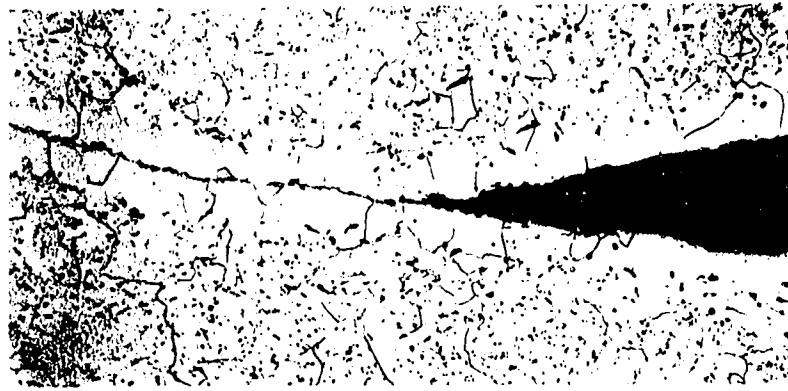
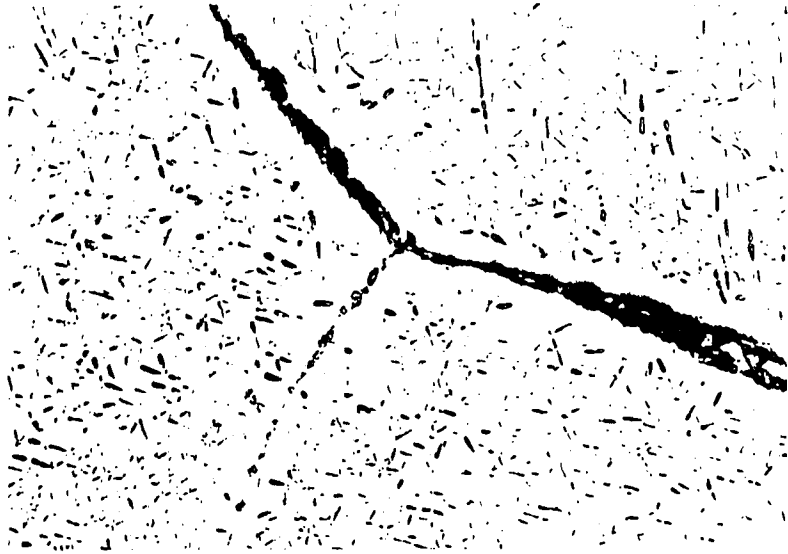


Figure 34. Photomicrographs illustrating intergranular fracture in vanadium containing:  
(a) 3400 ppm carbon  
(b) 4500 ppm carbon  
(c) 5700 ppm carbon  
X100



carbon alloys. No twinning at low temperatures was found in any specimens containing a second phase, that is above 300 ppm carbon. These observations suggest that twinning is suppressed by the presence of precipitates; hence by annealing at a sufficiently high temperature and by quenching rapidly to retain the carbon in solid solution twinning might be observed in these alloys. To test this supposition a series of specimens containing up to 1200 ppm carbon were heated to 1430°C, held for 3 hours and quenched in a cold brine solution. The specimens were examined and no evidence of quenching twins was observed. The specimens were then tested at -196°C and all were found to contain a number of mechanical twins. From these observations it is concluded that dispersed particles inhibit twinning in vanadium either by providing sites for stress relaxation or by acting as sources for the formation of glide dislocations.

## VI. SUMMARY

The deformation behavior of vanadium was examined by means of tensile specimens tested in the temperature range in which vanadium exhibited strain aging and by means of bend specimens tested in the temperature range in which vanadium exhibited a brittle-ductile transition.

The experimental results of this study show rather clearly that nitrogen is associated with the strain aging effects observed in vanadium.

The following strain-aging characteristics were observed in this investigation:

- (i) Maxima in the tensile strength and strain hardening exponent.
- (ii) Minima in the strain-rate sensitivity and uniform elongation.
- (iii) Occurrence of serrations in the stress-strain curve.
- (iv) The return of the yield point after an appropriate strain and aging treatment.

The tensile strength versus temperature curves are characterized by the existence of a strain-aging peak, the magnitude of which is dependent upon the nitrogen content, and from an investigation of the strain rate dependence of

this peak an activation energy of  $37.3 \pm 3.7$  kcal/mole was calculated. This value is in good agreement with that determined for the diffusion of nitrogen in vanadium, thus relating the strain aging peak observed in vanadium to the diffusion of nitrogen atmospheres with moving dislocations.

Static strain aging in vanadium is characterized by the return-of-yield point, and an activation energy of  $36.2 \pm 4.5$  kcal/mole was determined for this phenomenon. This value is also in good agreement with that associated with the diffusion of nitrogen in vanadium, thus indicating that pinning of the dislocations by nitrogen is responsible for the occurrence of a yield point in vanadium.

Although nitrogen has a marked effect on the hardness of vanadium no embrittlement was produced in amounts below 2000 ppm. Above this concentration, however, embrittlement occurs and the brittle-ductile transition temperature increases with increasing nitrogen content. In the polycrystalline case cracks were observed to nucleate along grain boundaries. The brittle-ductile transition temperature for single crystals was 50 to 60°C lower than the transition temperature for polycrystalline specimens of the same nitrogen content. It is suggested that crack propagation is the controlling factor in

determining the brittle fracture of polycrystalline vanadium with grain boundaries serving as sources for crack nucleation and crack nucleation being the controlling factor in the single crystal case. No evidence was found to indicate that mechanical twinning was responsible for the embrittlement observed in vanadium.

The addition of 200 to 300 ppm carbon markedly increases the hardness and strength of vanadium with further additions having little appreciable influence upon these properties. Carbon does not produce a brittle-ductile transition in vanadium and when present as a dispersed second phase, suppresses mechanical twinning.

## VII. BIBLIOGRAPHY

1. Lincoln, R., G. Asai and H. Kato. Some properties of vanadium. U. S. Bureau of Mines Report of Investigations 5975. 1962.
2. Van Thyne, R. J. Vanadium alloys in aerospace. Journal of Metals 15: 642-644. 1963.
3. Hahn, G. T., A. Gilbert and R. I. Jaffee. The effects of solutes on the ductile-to-brittle transition in refractory metals. United States Atomic Energy Commission Report DMIC Memo 155 [Battelle Memorial Institute Defense Metals Information Center, Columbus, Ohio]. 1962.
4. Cottrell, A. H. Effect of solute atoms on the behavior of dislocations. In Report of a Conference on Strength of Solids, University of Bristol, July 7-9, 1947. pages 30-36. Physical Society, London. 1948.
5. Suzuki, H. Chemical interaction of solute atoms with dislocations. Tohoku University Research Institute Science Reports A4: 455-463. 1952.
6. Cottrell, A. H. Interactions of dislocations and solute atoms. In Relation of properties to microstructure. pages 131-162. American Society for Metals, Cleveland, Ohio. 1954.
7. Fisher, J. C. Short-range order hardening. Physical Review 91: 232. 1953.
8. Cottrell, A. H. and B. A. Bilby. Dislocation theory of yielding and strain ageing of iron. Proceedings of the Physical Society (London) 62A: 49-62. 1949.
9. Harper, S. Precipitation of carbon and nitrogen in cold worked alpha-iron. Physical Review 83: 709-712. 1951.
10. Thomas, W. R. and G. M. Leak. The strain ageing of alpha-iron. Journal of the Iron and Steel Institute 180: 155-161. 1955.

11. Wilson, D. V. and B. Russell. The contribution of precipitation to strain ageing in low carbon steels. *Acta Metallurgica* 8: 468-479. 1960.
12. Barrand, P. and G. M. Leak. On the density of dislocation atmospheres. *Acta Metallurgica* 11: 158-160. 1963.
13. Nabarro, F. R. N. Mechanical effects of carbon in iron. In Report of a Conference on Strength of Solids, University of Bristol, July 7-9, 1947. pages 38-45. Physical Society, London. 1948.
14. Cochardt, A. W., G. Schoeck and H. Wiedersich. Interaction between dislocations and interstitial atoms in body-centered cubic metals. *Acta Metallurgica* 3: 533-537. 1955.
15. Hedges, J. M. and J. W. Mitchell. The observation of polyhedral sub-structures in crystals of silver bromide. *Philosophical Magazine* 44: 223-224. 1953.
16. Hedges, J. M. and J. W. Mitchell. Some experiments on photographic sensitivity. *Philosophical Magazine* 44: 357-388. 1953.
17. Mitchell, J. W. Precipitation reactions in crystals of silver and alkali halides. *Discussions of the Faraday Society* 28: 242-247. 1959.
18. Dash, W. C. Copper precipitation on dislocations in silicon. *Journal of Applied Physics* 27: 1193-1195. 1956.
19. Phillips, V. A. An electron microscopic study of quenching and strain-aging in a dilute Fe-C-N alloy. *Transactions Quarterly of the American Society for Metals* 56: 600-617. 1963.
20. Van Wijk, F. and J. A. B. Van Dijk. Investigation of pure iron and soft steel with the electron microscope. *Acta Metallurgica* 4: 657-659. 1956.

21. Phillips, V. A. New evidence for segregation at grain boundaries, subgrain boundaries and dislocations in dilute iron-carbon-nitrogen alloys. *Acta Metallurgica* 11: 1139-1150. 1963.
22. Weissmann, S. Investigation of crystalline imperfections and properties of materials. *American Scientist* 51: 193-226. 1963.
23. Lubahn, J. D. Strain aging effects. *Transactions of the American Society for Metals* 44: 643-664. 1952.
24. Hundy, B. B. The strain-age hardening of mild steel. *Metallurgia* 53: 203-211. 1956.
25. Ingram, A. G. Strain aging of refractory metals. United States Atomic Energy Commission Report DMIC 134 [Battelle Memorial Institute Defense Metals Information Center, Columbus, Ohio]. 1960.
26. Kabler, M. N., M. G. Miller and L. M. Slifkin. Dislocation-impurity interactions and strain aging in AgCl. *Journal of Applied Physics* 34: 1953-1957. 1963.
27. Brown, L. M. and P. L. Pratt. Strain ageing in CdCl<sub>2</sub>-doped rock salt. *Philosophical Magazine* 8: 717-734. 1963.
28. Cottrell, A. H. and C. M. Leak. Effect of quench aging on strain aging in iron. *Journal of the Iron and Steel Institute* 172: 301-306. 1952.
29. Jones, B. and R. A. Owen-Barnett. The strain-ageing of pure iron. *Journal of the Iron and Steel Institute* 180: 20-23. 1955.
30. Butler, J. F. Identification and stability of BN in boron low-carbon steels. *Transactions of the Metallurgical Society of the American Institute of Mining, Metallurgical and Petroleum Engineers* 224: 84-89. 1962.
31. Butler, J. F. The effect of heat treatment and microstructure on carbon strain aging in low carbon steels.

Transactions of the Metallurgical Society of the American Institute of Mining, Metallurgical and Petroleum Engineers 224: 89-96. 1962.

32. Fraser, R. W. and J. A. Lund. Effect of titanium additions on the low-temperature behavior of vanadium. Canadian Metallurgical Quarterly 1: 1-11. 1962.
33. Helsop, J. and N. J. Petch. The stress to move a free dislocation in alpha iron. Philosophical Magazine 1: 866-873. 1956.
34. Schoeck, G. On the yield stress in body-centered cubic metals. Acta Metallurgica 9: 382-383. 1961.
35. Stein, D. F., J. R. Low, Jr., and A. U. Seybolt. The mechanical properties of iron single crystals containing less than  $5 \times 10^{-3}$  ppm carbon. General Electric Research Laboratory (Schenectady, New York) Report 63-RL-3279M. 1963.
36. Blewitt, T. H., R. R. Coltman and J. K. Redman. Low-temperature deformation of copper single crystals. Journal of Applied Physics 28: 651-660. 1957.
37. Boniszewski, T. and G. C. Smith. The influence of hydrogen on the plastic deformation ductility, and fracture of nickel in tension. Acta Metallurgica 11: 165-178. 1963.
38. Cottrell, A. H. A note on the Portevin-leChatelier effect. Philosophical Magazine 44: 829-832. 1953.
39. Wessel, E. T., L. L. France and R. T. Begley. The flow and fracture characteristics of electron-beam-melted columbium. In Douglass, D. L. and F. W. Kunz, editors. Columbium metallurgy. Volume 10. pages 459-502. Interscience Publishers, New York. 1961.
40. Weaver, C. W. Tensile properties of annealed chromium between -196 and +900°C. Journal of the Institute of Metals 89: 385-390. 1961.
41. Pugh, J. W. Temperature dependence of the tensile properties of vanadium. Transactions of the Metallurgical Society of the American Institute of Mining, Metallurgical and Petroleum Engineers 209: 1243-1244. 1957.

42. Farrell, J. W. Mechanical properties of unalloyed vanadium. Transactions Quarterly of the American Society for Metals 54: 143-157. 1961.
43. Eustice, A. L. and O. N. Carlson. Effect of hydrogen on the tensile properties of iodide vanadium. Transactions of the Metallurgical Society of the American Institute of Mining, Metallurgical and Petroleum Engineers 221: 238-241. 1961.
44. Bradford, S. A. and O. N. Carlson. The role of oxygen in strain aging of vanadium. Transactions of the Metallurgical Society of the American Institute of Mining, Metallurgical and Petroleum Engineers 224: 738-742. 1962.
45. Shank, M. E. A critical survey of brittle failure in carbon steel structures other than ships. American Society for Testing Materials Special Technical Publication 158: 45-108. 1954.
46. Schwartzberg, F. R., H. R. Ogden and R. I. Jaffee. Ductile-brittle transition in the refractory metals. United States Atomic Energy Commission Report DMIC 114 [Battelle Memorial Institute Defense Metals Information Center, Columbus, Ohio]. 1959.
47. Ingram, A. G., E. S. Bartlett and H. R. Ogden, Effect of  $O_2$  and  $H_2$  on the mechanical properties of tantalum and columbium at low temperatures. Transactions of the Metallurgical Society of the American Institute of Mining, Metallurgical and Petroleum Engineers 227: 131-136. 1963.
48. Bechtold, J. H. and H. Scott. Mechanical properties of arc-cast and powder metallurgy molybdenum. Journal of the Electrochemical Society 98: 495-504. 1951.
49. Bechtold, J. H. and P. G. Shewmon. Flow and fracture characteristics of annealed tungsten. Transactions of the American Society for Metals 46: 397-408. 1954.
50. Roberts, B. W. and H. C. Rogers. Observations on mechanical properties of hydrogenated vanadium. Transactions of the Metallurgical Society of the American Institute of

- Mining, Metallurgical and Petroleum Engineers 206: 1213-1215. 1956.
51. Clough, W. R. and A. S. Pavlovic. The flow, fracture, and twinning of commercially pure vanadium. Transactions of the American Society for Metals 52: 948-970. 1960.
  52. Loomis, B. A. and O. N. Carlson. Investigation of the brittle-ductile transition in vanadium. In Clough, W. R., editor. Reactive metals. Volume 2. pages 227-243. Interscience Publishers, New York. 1959.
  53. Bradford, S. A. and O. N. Carlson. Effect of oxygen on the lattice constant, hardness and ductility of vanadium. Transactions Quarterly of the American Society for Metals 55: 169-178. 1962.
  54. Magnusson, A. W. and M. W. Baldwin, Jr. Low temperature brittleness. Journal of the Mechanics and Physics of Solids 5: 172-181. 1957.
  55. Armstrong, W. M. and J. A. H. Lund. Studies of the low-temperature tensile properties of some refractory metals. Canadian Mining and Metallurgical Bulletin 64: 305-310. 1961.
  56. Griffith, A. A. The phenomena of rupture and flow in solids. Philosophical Transactions of the Royal Society of London 221A: 163-198. 1920.
  57. Ludwik, P. Die bedeutung des gleit und reisswiderstandes für die werkstoff prüfung. Zeitschrift Verein Deutscher Ingenieure 71: 1532-1538. 1927.
  58. Zener, C. The micro-mechanisms of fracture. In Fracturing of metals. pages 3-31. American Society for Metals, Cleveland, Ohio. 1948.
  59. Stroh, A. N. The formation of cracks as a result of plastic flow. Proceedings of the Royal Society of London 223A: 404-414. 1954.

60. Cottrell, A. H. Theory of brittle fracture in steel and similar metals. Transactions of the Metallurgical Society of the American Institute of Mining, Metallurgical and Petroleum Engineers 212: 192-203. 1958.
61. Stroh, A. N. The cleavage of metal single crystals. Philosophical Magazine 3: 597-606. 1958.
62. Stokes, R. J., T. L. Johnston and C. H. Li. The relationship between plastic flow and the fracture mechanism in magnesium oxide single crystals. Philosophical Magazine 4: 920-932. 1959.
63. Stokes, R. J., T. L. Johnston and C. H. Li. Effect of slip distribution on the fracture behavior of magnesium oxide single crystals. Philosophical Magazine 6: 9-24. 1961.
64. Johnston, T. L., R. J. Stokes and C. H. Li. Crack reduction in magnesium oxide bi-crystals under compression. Philosophical Magazine 7: 23-34. 1962.
65. Honda, R. Cleavage fracture in single crystals of silicon iron. Journal of the Physical Society of Japan 16: 1309-1321. 1961.
66. Hornbogen, E. Dynamic effects during twinning in alpha iron. Transactions of the Metallurgical Society of the American Institute of Mining, Metallurgical and Petroleum Engineers 221: 711-715. 1961.
67. Hull, D. Twinning and fracture of single crystals of 3% silicon iron. Acta Metallurgica 8: 11-18. 1960.
68. McHargue, C. J. and H. E. McCoy. Effect of interstitial elements on twinning in columbium. Transactions of the Metallurgical Society of the American Institute of Mining, Metallurgical and Petroleum Engineers 227: 1170-1174. 1963.
69. McNeil, J. F. and H. R. Limb. Cleavage fracture in cast chromium of high purity. Journal of the Institute of Metals 87: 79-87. 1958.

70. Hook, R. E. and A. M. Adair. On the recrystallization embrittlement of chromium. Transactions of the Metallurgical Society of the American Institute of Mining, Metallurgical and Petroleum Engineers 227: 151-159. 1963.
  71. Bechtold, J. H. Cleavage in the refractory metals. In Averback, B. L., D. K. Felbeck, G. T. Hahn and D. A. Thomas, editors. Fracture. pages 628-638. John Wiley and Sons, Incorporated, New York. 1959.
  72. Carlson, O. N. and C. V. Owen. Preparation of high-purity vanadium metal by the iodide refining process. Journal of the Electrochemical Society 108: 88-93. 1961.
  73. Allen, N. P., O. Kubaschewski and O. Von Goldbeck. The free energy diagram of the vanadium-oxygen system. Journal of the Electrochemical Society 98: 417-424. 1951.
  74. Keh, A. S. and W. C. Leslie. Recent observations on quench-aging and strain-aging of iron and steel. United States Steel Corporation Research Center (Monroeville, Pennsylvania) Report 1011. 1962.
  75. Carreker, R. P., Jr. Plastic flow of platinum wires. Journal of Applied Physics 21: 1289-1296. 1950
  76. Tichelaar, G. W., R. V. Coleman and D. Lazarus. Effect of pressure on the mobility of interstitial oxygen and nitrogen in vanadium. Physical Review 121: 748-752. 1961.
  77. Powers, R. W. Internal friction in oxygen-vanadium and nitrogen-vanadium solid solutions. Acta Metallurgica 2: 604-607. 1954.
  78. Powers, R. W. and M. V. Doyle. Diffusion of interstitial solutes in the group Va transition metals. Journal of Applied Physics 30: 514-524. 1959.
  79. Powers, R. W. and M. V. Doyle. The diffusion of carbon and oxygen in vanadium. Acta Metallurgica 6: 643-646. 1958.
-

80. Stanley, J. T. and C. A. West. Internal friction of interstitial solid solutions of oxygen and nitrogen in vanadium. *Acta Metallurgica* 3: 107-108. 1955.
81. Bolling, G. F. Yield point phenomena in alpha brass and other face-centered cubic metals. *Philosophical Magazine* 4: 537-559. 1959.
82. Cowgill, D. S. Deformation behaviors of niobium and tantalum at low temperatures. Unpublished Ph.D. thesis. Library, Iowa State University of Science and Technology, Ames, Iowa. 1964.

## VIII. ACKNOWLEDGEMENTS

The author wishes to express his sincere appreciation to Professor O. N. Carlson whose helpful counsel and guidance have been primarily responsible for the success of this study. The author is also indebted to C. V. Owen and F. A. Schmidt for materials and fabrication, H. Baker and E. Hopkins for metallographic services, and A. Pappas for assistance in specimen preparation and testing.